FLEXIBLE SERS SUBSTRATE FABRICATED FROM GOLD NANOSTAR

Miss Piboonwan Insiti

จุฬาลงกรณ์มหาวิทยาลัย
CHULALONGKORN UNIVERSITY

A Thesis Submitted in Partial Fulfillment of the Requirements
for the Degree of Master of Science in Chemistry
Department of Chemistry
FACULTY OF SCIENCE
Chulalongkorn University
Academic Year 2019

เซอรส์ซับสเตรตชนิดยืดหยุ่นขึ้นรูปจากโกลด์นาโนสตาร์

น.ส.พิบูลย์วรรณ อินสิติ

Thesis Title	FLEXIBLE SERS SUBSTRATE FABRICATED FROM GOLD NANOSTAR
By	Miss Piboonwan Insiti
Field of Study	Chemistry
Thesis Advisor	Professor SANONG EKGASIT, Ph.D.

Accepted by the FACULTY OF SCIENCE, Chulalongkorn University in Partial Fulfillment of the Requirement for the Master of Science

.... Dean of the FACULTY OF SCIENCE

    ()

THESIS COMMITTEE

.... Chairman
    (Associate Professor VUDHICHAI PARASUK, Ph.D.)

.... Thesis Advisor
    (Professor SANONG EKGASIT, Ph.D.)

.... Examiner
    (Professor SUMRIT WACHARASINDHU, Ph.D.)

.... External Examiner
    (Chaweewan Sapcharoenkun, Ph.D.)

จุฬาลงกรณ์มหาวิทยาลัย

CHULALONGKORN UNIVERSITY

พิบูลย์วรรณ อินสิติ : เซอร์สซับสเตรตชนิดยืดหยุ่นขึ้นรูปจากโกลด์นาโนสตาร์. (FLEXIBLE SERS SUBSTRATE FABRICATED FROM GOLD NANOSTAR) อ.ที่ปรึกษาหลัก : ศ. ดร.สนอง เอกสิทธิ์

ในงานวิจัยนี้คณะนักวิจัยสนใจพัฒนาวิธีการขึ้นรูปแผ่นรองรับขยายสัญญาณรามานที่สามารถทำได้ง่ายในขั้นตอนเดียว โดยมีอนุภาคทองคำระดับนาโนเมตรรูปเสมือนทรงกลมกระจายตัวอย่างสม่ำเสมอบนแผ่นรองรับแบบกลมเส้นผ่านศูนย์กลาง 5 มิลลิเมตร พื้นผิวของกระดาษกรองถูกเคลือบด้วยแบคทีเรียเซลลูโลสนาโนคริสตัลทำให้พื้นผิวเรียบขึ้น โดยแบคทีเรียเซลลูโลสนาโนคริสตัลคอลลอยด์เข้าไปเติมเต็มช่องว่างระหว่างเส้นใยของกระดาษกรองและสร้างฟิล์มบางขึ้น อนุภาคทองคำระดับนาโนเมตรรูปเสมือนทรงกลมถูกสังเคราะห์บนฟิล์มแบคทีเรียเซลลูโลสนาโนคริสตัลโดยตรงผ่านกระบวนการสังเคราะห์ด้วยวิธีการปลูกเม็ด โดยฟิล์มแบคทีเรียเซลลูโลสนาโนคริสตัลที่มีหมู่ไฮดรอกซิลจำนวนมากช่วยตรึงอนุภาคทองคำระดับนาโนเมตร ส่งผลให้อนุภาคทองคำระดับนาโนเมตรรูปเสมือนทรงกลมมีการกระจายตัวอย่างสม่ำเสมอ แผ่นรองรับขยายสัญญาณรามานที่พัฒนาขึ้นถูกนำมาทดสอบประสิทธิภาพในการช่วยเพิ่มความเข้มของสัญญาณ และความสม่ำเสมอของสัญญาณรามาน โดยใช้ 4-อะมิโนไทโอฟีนอลเป็นสารวิเคราะห์ จากผลการทดลองสามารถบ่งชี้ได้ว่าการกระจายตัวอย่างสม่ำเสมอของอนุภาคทองคำระดับนาโนเมตรรูปเสมือนทรงกลมบนแผ่นรองรับกระดาษกรองที่ถูกเคลือบด้วยแบคทีเรียเซลลูโลสนาโนคริสตัลส่งผลให้ความเข้มสัญญาณรามานที่ตำแหน่ง 1079 cm^{-1} สูงขึ้นจาก 1349 cps เป็น 4600 cps ในขณะที่ค่าส่วนเบี่ยงเบนมาตรฐานสัมพัทธ์ของความเข้มสัญญาณลดลงจาก 30.3% เหลือเพียง 8.9% เมื่อเทียบกับกระดาษกรองที่ไม่ได้เคลือบด้วยแบคทีเรียเซลลูโลสนาโนคริสตัล ความเข้มข้นต่ำสุดของ 4-อะมิโนไทโอฟีนอลที่สามารถวัดได้คือ 1 นาโนโมลาร์ อีกทั้งยังสามารถตรวจวิเคราะห์สารปริมาณน้อยของสารกำจัดศัตรูพืชไทแรมได้ต่ำถึง 0.134 พิโคโมลาร์ แผ่นรองรับขยายสัญญาณการกระเจิงรามานชนิดยืดหยุ่นช่วยทำให้สัญญาณรามานมีความเข้มสูง และสม่ำเสมอขึ้น สามารถเตรียมได้ง่ายในห้องปฏิบัติการทั่วไป ใช้งานง่าย มีความเสถียรสูง และต้นทุนต่ำ มีศักยภาพในการตรวจวัดสารเคมีปริมาณน้อย

สาขาวิชา   เคมี   ลายมือชื่อนิสิต ....

ปีการศึกษา   2562   ลายมือชื่อ อ.ที่ปรึกษาหลัก ....

In this work, a one-pot protocol for the fabrication of surface-enhanced Raman scattering (SERS) substrate has been developed. It consists of quasi-spherical gold nanoparticles (AuQNPs) uniformly which is deposited on a disk paper substrate (5-mm in diameter). The disk of filter paper surface was coated by bacterial cellulose nanocrystal (BCNC). The BCNC smoothed the surface by forming thin nanopaper film upon drying while filling the gap between fibers. AuQNPs was directly synthesized on the surface of BCNC film via seed-growth method. The BCNC film with abundant hydroxyl groups became anchor points for AuNPs which help to create uniform distribution of AuQNP. The performance of the developed SERS substrate was evaluated by 4-aminothiophenol (4-ATP). The results indicated that the uniform distribution of AuQNP on BCNC/filter-paper SERS substrate leads to an increase of the SERS intensity at 1079 cm^{-1} of 4-ATP from 1348 cps to 4600 cps while the relative standard deviation (RSD) was decreased from 30.3% to 8.9% compared to AuQNP/filter-paper SERS substrate. The lowest concentration of 4-ATP that can be detected was 1 nM. Furthermore, AuQNP/BCNC/filter-paper substrate can detect trace thiram pesticide with the limit of detection at 0.134 pM. The experiment would be an effective technique for preparing flexible SERS substrates that easily prepared in laboratory. This disposable, reproducible, highly stable, easy to use and low-cost SERS substrate, which affords high intensity and uniform SERS signal, has potential for trace chemical detection in practical application.

จุฬาลงกรณ์มหาวิทยาลัย
CHULALONGKORN UNIVERSITY

Field of Study: Chemistry   Student's Signature
                                         ....
Academic   2019   Advisor's Signature
Year: ....

ACKNOWLEDGEMENTS

TABLE OF CONTENTS

Page

LIST OF TABLES

Page

LIST OF FIGURES

จุฬาลงกรณ์มหาวิทยาลัย

CHULALONGKORN UNIVERSITY

LIST OF STMBOLS AND ABBREVIATIONS

λ_{max}	: wavelength at which maximum absorption occurs in nm
ϕ	: diameter
4-ATP	: 4-aminothiophenol
Ag	: silver
AgNPs	: silver nanoparticles
$AgNO_3$	: silver nitrate
Au	: gold
AuNPs	: gold nanoparticles
AuQNPs	: quasi-spherical gold nanoparticles
BCNC	: bacterial cellulose nanocrystal
cm^{-1}	: wavenumber
cps	: counts per second
DI	: deionized
CNF	: cellulose nanofibrils
EtOH	: ethanol
et al.	: et al ii, in Latin meaning "and others"
e.g.	: exempli gratia, in Latin meaning "for example"
FE-SEM	: field emission scanning electron microscope
FTIR	: fourier transform infrared
h	: hour
H_2O_2	: hydrogen peroxide
I_{avg}	: average intensity
LSPR	: localized surface plasmon resonance
min	: minute
μm	: micrometer
mm	: milimeter
mL	: milliliter
μL	: microliter
M	: molar

mM	: millimolar
μM	: micromolar
nM	: nanomolar
nm	: nanometer
NPs	: nanoparticles
OM	: optical microscope
pM	: picomolar
Pt	: platinum
PDMS	: polydimethylsiloxane
RSD	: relative standard deviation
SEM	: scanning electron microscope
SERS	: surface-enhanced Raman scattering
TEM	: transmission electron microscope
UV-Vis	: ultraviolet-visible
V/m	: volts per meter

CHAPTER 1

INTRODUCTION

1.1 Research background

In an analysis of residual pesticides in foods, water and agricultural products, surface-enhanced Raman scattering (SERS) has become a powerful and attractive spectroscopic technique because it is a rapid and sensitive analytical tool for an identification of chemicals [1-3]. This technique is widely used for low-concentration and trace chemical sensing using noble metal nanoparticles (Ag, Au or Pt) as substrate to enhance the Raman scattering intensity [4, 5]. Gold nanoparticles (AuNPs) have been extensively studied in SERS applications because of low toxicity and chemically inert which offer great environmental safety and high stability [6]. The effectiveness of nanoparticles in enhancing Raman scattering intensity is strongly dependent on shape and size of metal nanoparticles. In addition, nanogaps and aggregations of metal nanoparticles also play a key role in SERS enhancement [7-9]. For molecular detection with SERS, the metal nanoparticles should be initially used in the form of colloid. However, there is a limitation using the colloidal metal as the substrate for SERS sensing due to inconvenience in handling and uncontrollable metal aggregation affecting the reproducibility of SERS signal. To overcome this problem, nanoparticles are fabricated on a solid substrate to easily control particle aggregation in order to obtain easy-to-use SERS substrate [10].

Nowadays, solid-phase substrates such as silicon, glass, polydimethylsiloxane (PDMS), and filter paper are extensively used for the fabrication of SERS substrates [11-15]. For real practical applications, a disposable and flexible SERS substrate with high enhancement, uniform signal, and long-shelf-life is essential. Filter paper-based gold nanoparticle is one of the alternative materials for the fabrication of SERS substrate because filter paper is lightweight, flexible, portable, low cost, and generally available in laboratories. In particular, with an advantage of a large surface area and high porosity, filter paper can allow high adsorption of metal nanoparticles which is useful for the enhancement of Raman scattering intensity [16]. Various methods had been reported to fabricate filter paper-based SERS substrate, including, thermal inkjet

printing [17], physical vapor deposition [18, 19], immobilization [20], solution dipping [21], drop-casting [22, 23] and dip coating [24]. Among these fabrication methods, inkjet printing and physical vapor deposition were found to be the most effective methods for the deposition of metal nanoparticles on the substrate. However, the limitation of both methods is the requirement of a special instrument. Although the fabrication with the other methods provides an easier process and does not require any instrument, the problem on surface functionalization and time still remains. Most of these methods require at least two steps for fabrication including a synthesis of colloidal nanoparticle and a deposition of colloidal nanoparticles onto a substrate. Herein, the most challenging in the deposition of metal nanoparticles is a stability of colloidal nanoparticles. Generally, colloidal nanoparticles are not stable in solution thus there is difficulty in distributing them homogeneously over the substrate. During the synthesis, a stabilizer or a capping agent is added into the system to avoid the aggregation of particles, however, this process can interfere with the SERS signal because SERS is highly sensitive to chemical molecules. Thus, metal nanoparticles must possess a clean surface. In order to lessen the steps in the preparation and surface interference, the nanoparticles should be directly grown on the substrate using green chemistry approach. Recently, A. Pangdam developed a simple one-pot protocol to synthesize gold nanoparticles including urchin-like gold microstructure (UL-AuMS) and quasi-spherical gold nanoparticles (AuQNPs) by using hydrogen peroxide (H_2O_2) as a reducing agent [25]. This approach consumed less energy because the reaction was reacted at room temperature and the reaction was completed within 5 minutes. Hence, this approach is promising for producing a ready-to-use SERS substrate. Since there is no need of a stabilizer or capping agent, the surface of gold nanoparticles was pure.

In this work, we develop the simple one-pot protocol for the fabrication of ready-to-use SERS substrates by the direct growth of AuQNPs on a 5-mm filter paper disk via seed-growth method. AuQNPs were synthesized using H_2O_2 as a reducing agent. Furthermore, we attempt to increase uniform SERS signal by coating the filter paper with bacterial cellulose nanocrystal (BCNC). The BCNC was employed to fill pores and increase the surface smoothness of the filter paper, creating a uniform hot spot and uniform SERS signal. Our developed filter paper-based SERS substrate shows excellent SERS activity with uniform SERS signal, as we verify by adsorbing 4-ATP

on the surface and recording the SERS map. In addition, this highly sensitive SERS substrate has a potential to detect trace pesticide (thiram), which applicable to the real-world problem.

1.2 Objective

To develop the simple one-pot protocol for fabricating quasi-spherical gold nanoparticles (AuQNPs) on paper-based SERS substrate.

1.3 Scope of this research

1. To study the influence of seed-growth method to AuQNP synthesis.
2. To fabricate AuQNPs on filter paper and BCNC-coated filter paper for use as SERS substrate.
3. To characterize the morphology of AuQNPs.
4. To study SERS enhancement and signal uniformity of the developed filter paper-based SERS substrate by using 4-ATP as analyte molecules.
5. To demonstrate the application of the developed filter paper-based SERS substrate as a sensor for trace levels of thiram pesticides.

1.4 The benefit of this research

The developed filter paper-based SERS substrate will be used for trace level detection of pesticides under Raman microscope.

CHAPTER 2
THEORETICAL BACKGROUND

2.1 Surface-enhance Raman scattering (SERS)

Raman spectroscopy is a vibrational spectroscopic technique used for identifying chemicals through its vibrational patterns of functional groups of molecules (Molecular fingerprint). Raman spectroscopy technique observes the shift in wavelength through detecting the scattered light after interacting with the sample molecules and resulting in Raman spectral pattern, due to the vibrational modes of the molecules. The different functional groups provide different characteristic vibrational energies. Each substance has a unique Raman spectral pattern. However, Raman intensity is normally quite weak because only about 0.001% of the incident photons produce inelastic Raman scattering while 99.999% of incident photons produce elastic Rayleigh scattering in which useless for molecular characterization [26]. According to the spontaneous small intensity of Raman signal, a detection of low concentrations and trace of samples is hard to perform. In order to increase Raman intensity, surface-enhanced Raman scattering (SERS) technique was developed.

SERS is a spectroscopic technique that is exploited to increase Raman intensity of analyte molecules by using the noble metal nanoparticles as a substrate, as shown in Figure 2.1 [27, 28]. This technique is widely used in trace chemical detection. Gold nanoparticles and silver nanoparticles are attractive metal nanoparticles to construct SERS substrate for SERS sensing. When the scatter is placed on or near a roughened noble metal substrate, the Raman intensity is greatly enhanced. The enhancement of Raman signal relies on two contributions of chemical and electromagnetic enhancement effects [29, 30]. Chemical enhancement factor is arising from an excitation of adsorbate localized electronic resonances or metal-to-adsorbate charge-transfer resonance. The electromagnetic enhancement is the main parameter to give a large enhancement of Raman intensity. The enhancement occurs through localized surface plasmon resonance (LSPR) phenomenon. So, the nanostructured metal substrate is the key factor that controls the electromagnetic effect.
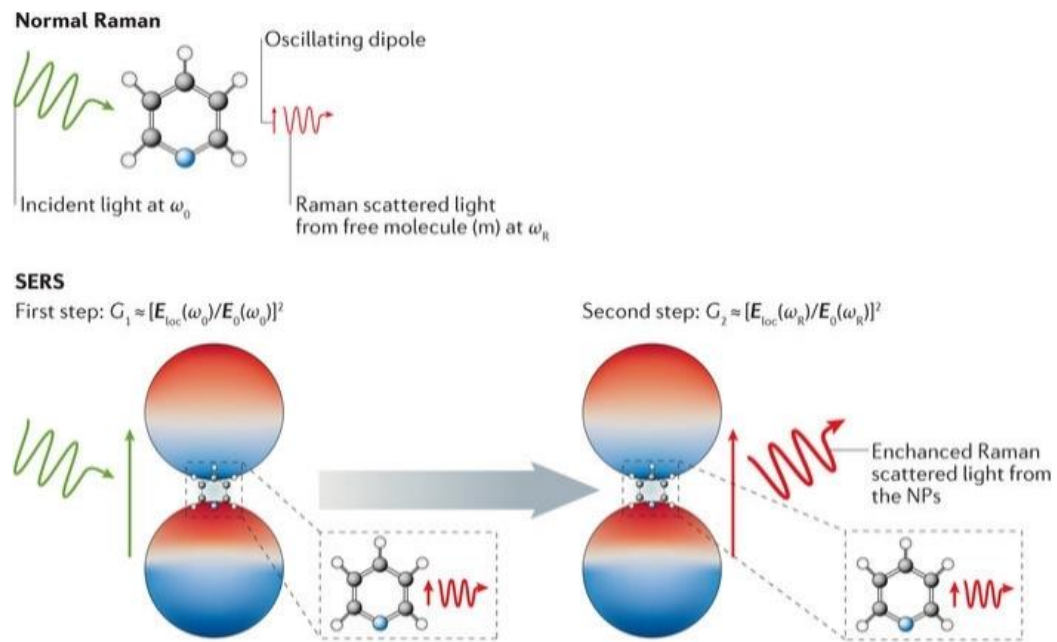
Figure 2.1 Principle of the surface-enhanced Raman scattering. Copyright 2016 Nature Publishing Group [27].

2.2 Localized surface plasmon resonance (LSPR)

Localized surface plasmon resonance (LSPR) is a coherent interaction between light and metal nanostructures, resulting in the collective oscillations of the surface electrons [26]. The enhancement of Raman signal occurs through LSPR phenomenon. Generally, electrons on the surface of metal nanoparticles (in nanoscale of particle size) are localized by quantum-size effect. The oscillation of electron cloud is called plasmon oscillation. When applying the external light which has the same frequency as electron clouds oscillating around metal surface, an electromagnetic field around the metal surface will be enhanced by resonance frequency between photon and plasmon as shown in Figure 2.2 [26]. According to plasmon resonance and inducing electric field enhancement around the metal surface, the scatter light effectively results in an increase of Raman intensity. Regarding an electromagnetic mechanism, an area where the electric field intensifies is called "hot spots" [31].
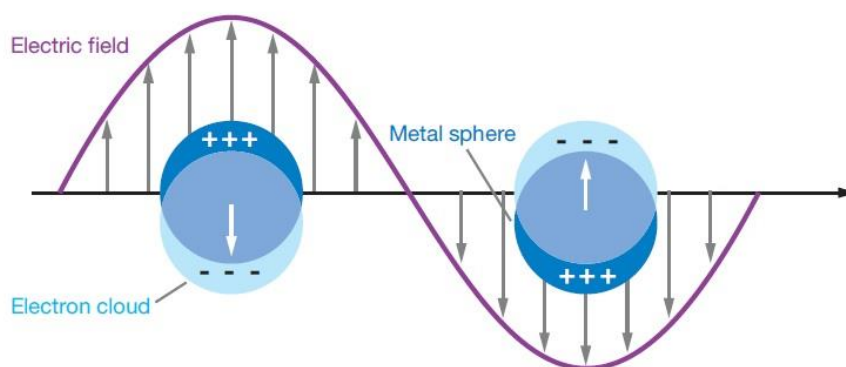
Figure 2.2 Schematic illustration of electron cloud oscillation generating localized surface plasmon resonance (LSPR) of metal nanospheres. Copyright 2007 Annual Review of Physical Chemistry [26].

The noble metal nanoparticles possess the strong LSPR properties. Gold and silver are commonly used because the oscillation frequencies of plasmons on the surfaces are high electrical conductivity, stable under diverse environment, ease of surface functionalization and optically tunable in visible region. With different size and shape, metal nanoparticles provide different LSPR properties. Besides, the junctions and gaps between two adjacent noble metal nanoparticles are affected. SERS enhancement is highly dependent on the plasmonic properties of metal nanostructures, which are determined by their size, shape, and aggregation state as well as their surrounding environment. Typically, the "hot spots" can be generated by single molecule or/and dimer of metal particle, as shown in Figure 2.3A. The most efficient hot spots are generated at the gaps between curved metallic surfaces, as shown in Figure 2.3B [26]. As consistent result with Figure 2.4, when the size of nanoparticle increased or the gap between particle decreased, the electric field is increased.
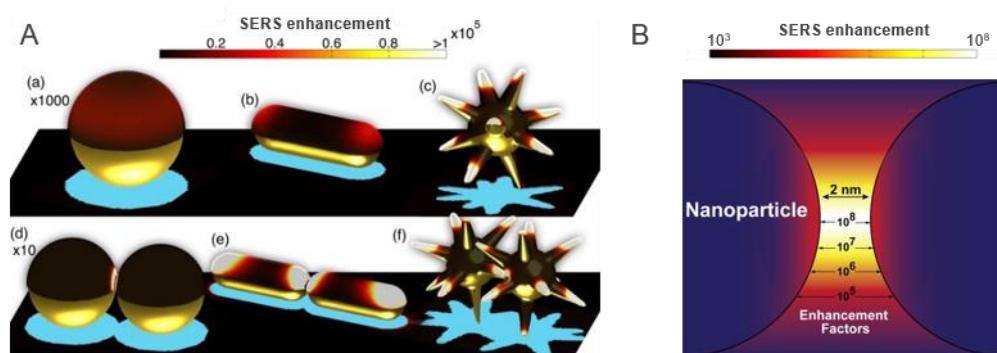
Figure 2.3   (A) Spatial distribution of the SERS enhancement on individual particle and dimer of particle. Copyright 2017 ACS Photonics [26]. (B) An illustration of "hot spot" for NP dimer and rapid change in SERS enhancement factors with respect to relative position. Copyright 2011 Analytica Chimica Acta [8].
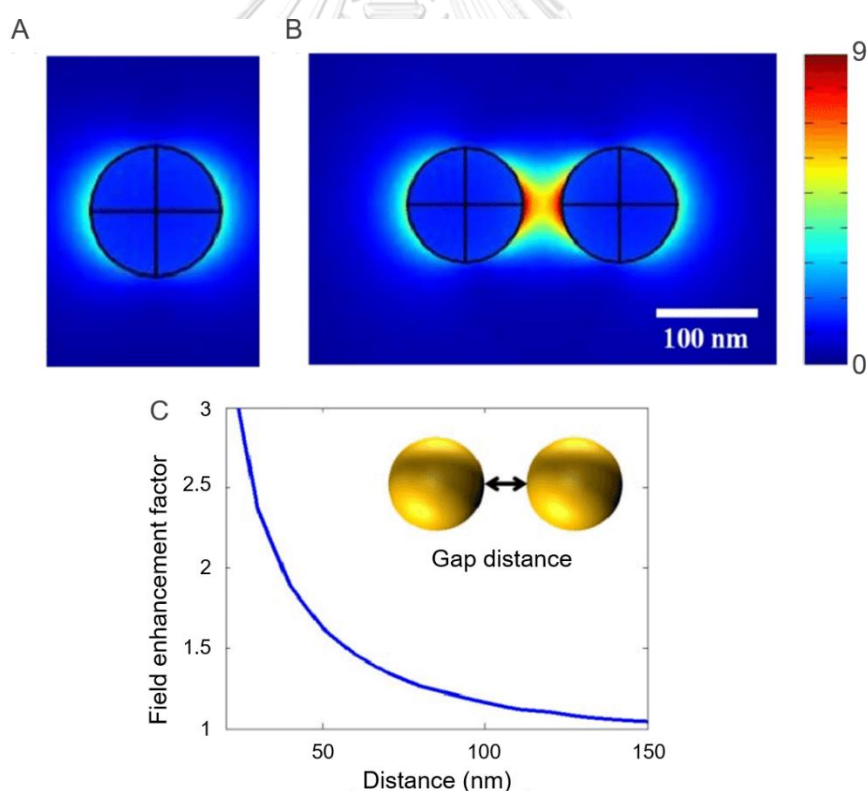
Figure 2.4   Electric field distributions (V/m) at (a) a single Au nanoparticle and (b) nanoparticle dimer. (c) Field enhancement factor of nanoparticle dimer with respect to the single nanoparticle. Copyright 2011 Sensor [32].

2.3 Gold nanoparticles for SERS application

SERS substrate from gold nanoparticles (AuNPs) has been extensively studied in SERS applications due to its wide tunable LSPR property, low toxicity, biocompatibility and long-term stability at room temperature [33]. The enhancement of Raman intensity is strongly dependent on the shape and size of the metal nanoparticles. The nanogap and aggregation of gold nanoparticles also play a key role in SERS enhancement. Too small (size < 20 nm) AuNPs provide a weaker Raman intensity enhancement for SERS application compared to the larger particle size [34, 35]. However, too large (> 120 nm) particles would not be suitable for the enhancement of Raman intensity. Therefore, an optimum particle size and packing density with nanoscale gaps will be affected [36, 37].

Seed-growth method is one of the alternative methods to control the growth system with an enlargement particle and narrow size distribution [38]. For example, Liu *et al.* synthesized different particle sizes of AuQNP via seed-growth method by varying $HAuCl_4$ concentration and using H_2O_2 as a reducing agent, as shown in Figure 2.5.
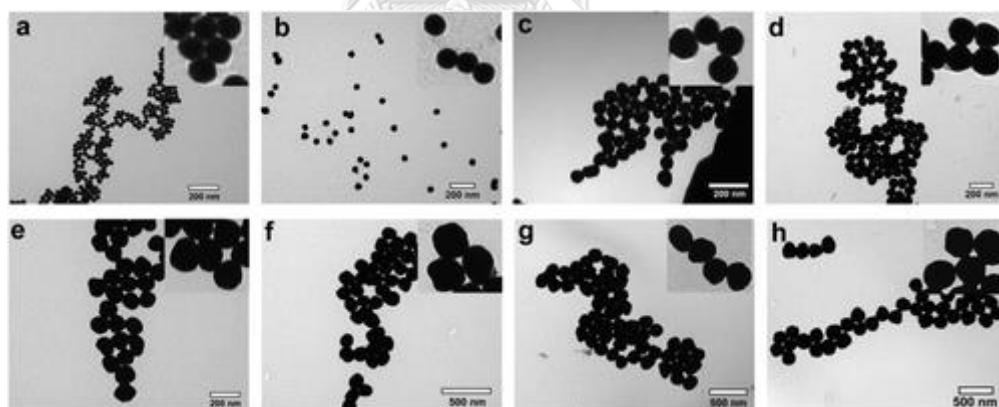
Figure 2.5   TEM images of Au NPs with sizes of (a) 32, (b) 48, (c) 68, (d) 81, (e) 120, (f) 147, (g) 190, and (h) 216 nm obtained by seed-growth method via H_2O_2 reduction of $HAuCl_4$. The high-magnification TEM images of the AuNPs are shown in the insets. Copyright 2012 American Chemical Society [38].

2.4 Fabrication of paper-based SERS substrate

Cellulose paper (e.g. filter paper, cellulose nanofibrils (CNF) nanopaper and bacterial nanocellulose hydrogel) is one of the most studied materials to make a SERS substrate due to it presents a low fluorescence signal and background [39, 40]. Furthermore, cellulose paper possesses the flexibility, high biocompatibility, high strength, abundant porosity, and large surface area which allow to absorb nanoparticles (NPs) on the surface. This thesis will concentrate on a literature review of filter paper.

In 2012, Fierro-Mercado, P. M. and Hernández-Rivera, S. P. fabricated filter-paper SERS substrate using thermal inkjet deposition method. According to their method, they used polyvinylpyrrolidone as a surfactant to stabilize nanoparticle in solution. Then AuNP was printed on filter paper via ImTech Imaging System model I-Jet 312S (ImTech, OR, USA), as shown in Figure 2.6. However, this method is required an instrument.
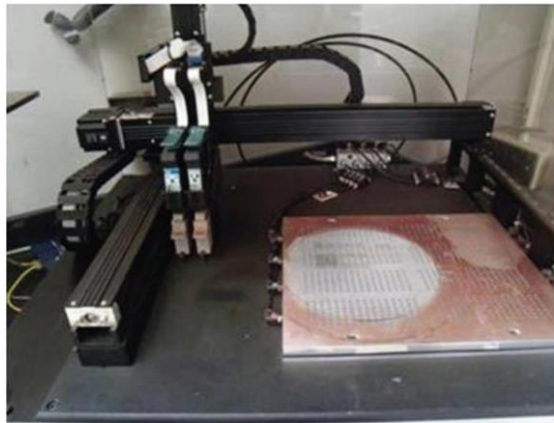
Figure 2.6   Photograph of thermal inkjet system used for preparing SERS substrates. Copyright 2012 International Journal of Spectroscopy [17].

In 2013, Ngo *et al.* used dipping method to prepare SERS substrate. The first step was the synthesis of AuNPs using tri-sodium citrate as a reducing agent. The second step was the preparation of filter paper substrates treated by aqueous solutions of cationic polyacrylamide (CPAM). The last step was the dipping of modified-filter paper into AuNPs solution, as shown in Figure 2.7. Cationic polyacrylamides with higher

bridging produced higher aggregation of AuNPs, resulting in excellent SERS reproducibility, sensitivity, and high enhancement factor. However, time-consuming and surface functionalization are required.
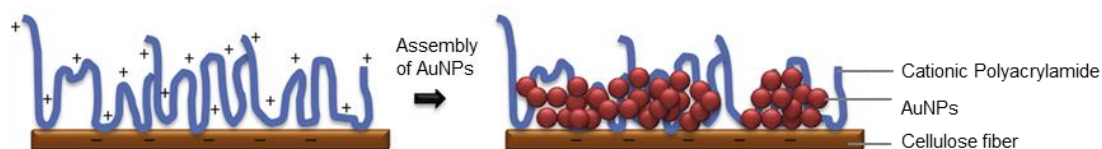
Figure 2.7 A schematic of AuNPs deposited on cationic polyacrylamide-treated filter paper. Copyright 2013 Colloid and Interface Science [41].

In 2018, Weng *et al.* developed SERS substrate using the inkjet-printing and seed-growth method, as shown in Figure 2.8. AuNPs were absorbed on the surface of filter paper due to the porosity of cellulose fibers and physical adsorption. Especially, filter paper contains a large number of the hydroxyl groups which facilitate the attachment of positively charged metal nanoparticles. This system is interesting which provides high SERS enhancement and uniform SERS signal, however, the expensive instrument is required.
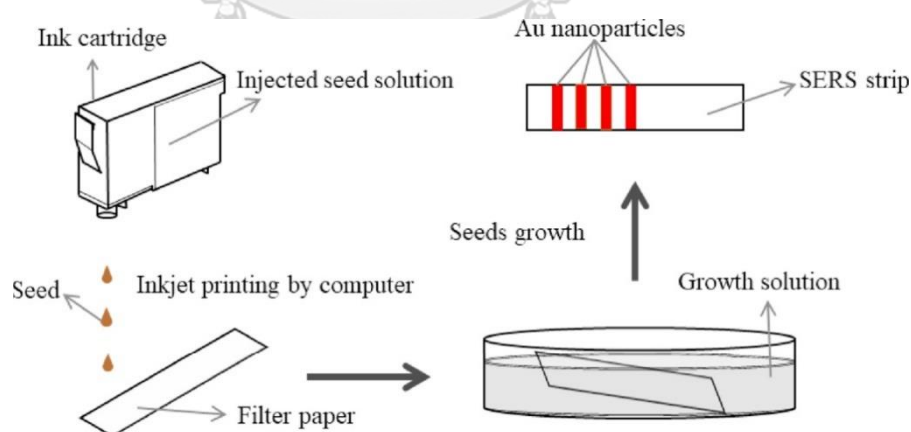
Figure 2.8 Schematic illustration of the preparation process of Au NP/paper strips. Copyright 2018 Solid State Communications [42].

Recently, nanocelluloses were employed to fill the pore and increase the surface smoothness of filter paper. In Figure 2.9, Oh *et al.* modified filter paper surface by

coating with cellulose nanofibrils (CNF) and then AgNP solution was dropped on CNF-coated filter paper which could decrease the local height differences, resulting in even distribution of AgNP and give higher uniform SERS signal [43]. However, this method requires multistep and need surface functionalization.
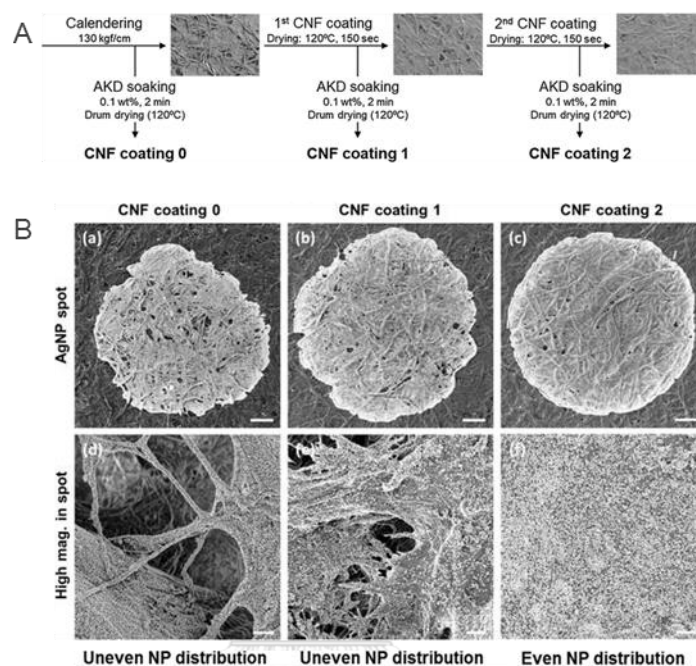
Figure 2.9 (A) Preparation process of CNF coated paper. (B) Characteristics of the AgNP spots, as observed by SEM: (Ba, Bd) before CNF coating, (Bb, Be) after first time CNF coating, and (Bc, Bf) after second time CNF coatings. Copyright 2013 Cellulose [43].

From above mentioned literature reviews, most of the fabrication methods required at least two steps and specific instruments. Herein, we had tried to fabricate the ready-to-use SERS substrate using one-pot synthesis. The filter paper surface coated by bacterial cellulose nanocrystal (BCNC) would be modified for increasing the surface smoothness. Then, BCNC-coated filter paper was used as substrate for a direct growth of AuQNP. We expected that it could be promoted an even distribution of AuQNP to obtain high enhancement and uniform SERS signal.

2.5 Bacterial cellulose nanocrystals (BCNC)

BCNC colloid is short nano-whiskers in solution, which shows birefringence effect as a unique property. BCNC, which were obtained from HCl-hydrolysis (Figure 2.10), provide pure cellulose with only hydroxyl groups that could not interfere the SERS detection. Generally, the BCNC can form into nanopaper film after drying, resulting from the irreversible collapse of the cellulose nanocrystalline network [44]. The nanopaper possesses thin film, transparent, non-toxic and inert. BCNC is a fragment of glucose nanofibrils obtained by hydrolysis at β-1,4 glycosidic bonds linking D-glucose which is similar to the chemical structure of cellulose of the filter paper [45]. According to remarkable chemical and physical properties of BCNC, the small dimension of BCNC can be used to fill the pore and formed a nanopaper thin film. This leads to higher surface smoothness of filter paper. Moreover, the surface of BCNC film with abundant hydroxyl groups helps to act as anchor points for AuNPs. Therefore, BCNC is a candidate material that is suitable to overcome the problem of filter paper roughness.
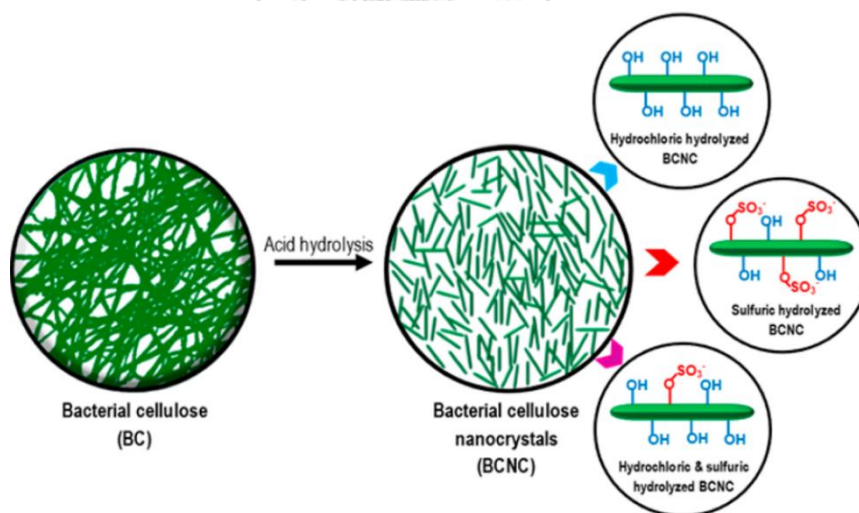
Figure 2.10 Schematic illustration of BCNC production from bacterial cellulose by acid hydrolysis with different types of acid. Copyright 2018 ACS Applied Nano Materials [45].

CHAPTER 3
EXPERIMENTAL SECTION

3.1 Chemicals and materials

1. 4-Aminothiophenol (4-ATP, C_6H_7NS, 97%), Sigma-Aldrich Co., Ltd.

2. Ammonium hydroxide (NH_4OH, 25% w/w), Merck Ltd.

3. Hydrogen peroxide (H_2O_2, 30% w/w), Merck Ltd.

4. Hydrochloric acid (HCl, 37% w/v), Merck Ltd.

5. Nitric acid (HNO_3, 25% w/w), Merck Ltd.

6. Silver nitrate ($AgNO_3$, purity $\geq$ 99.8%), Aencore Chemical Co., Ltd.

7. Sodium hydroxide (NaOH), Merck Ltd.

8. Tri-sodium citrate dehydrate ($Na_3C_6H_5O_7$, 99%), Carlo Erba Reagents S.A.S.

9. Tetrachloroauric (III) acid ($HAuCl_4$), Sigma-Aldrich Co., Ltd.

10. Filter paper (Grade 304, pore size 5-13 µm), Johnson test papers Ltd.

All chemicals were analytical grade and were used as received without any purification. In order to prepare the analyte solution for SERS measurement, ethanol was employed to dissolve 4-ATP, while the other chemicals were dissolved in milli-Q water. The deionized (DI) water was used for cleaning glassware. All glassware and magnetic bars were cleaned with detergent and soaked in aqua regia (a mixture of concentrated HCl and HNO_3 at a volume ratio of 3:1) for 30 min, rinsed with DI water several times, and with milli-Q water before using.

3.2 A procedure for gold nanoparticle synthesis

Gold nanoparticles (AuNPs) were synthesized using Turkevich method with some modifications [26], as shown in Figure 3.1. Briefly, $HAuCl_4$ solution (0.5 M, 25 µL) was added into milli-Q water (20 mL). The solution was heated until boiled under continuous stirring. Upon boiling, tri-sodium citrate solution (0.04 M, 2 mL) was rapidly added and continuously stirred until the solution turned into deep red wine

color. The solution was boiled and stirred for 10 min and then cooled to room temperature. The volume of the AuNPs colloidal solution was adjusted to 25 mL (the final concentration of gold ion was 0.5 mM).
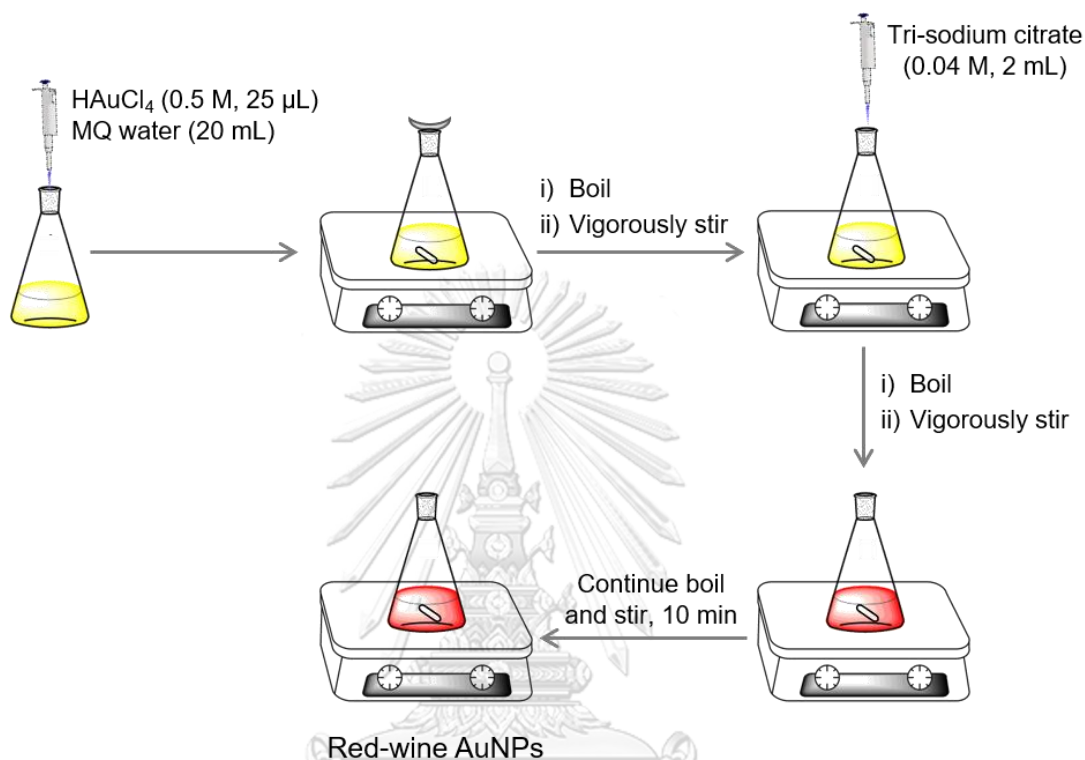
Figure 3.1   A schematic shows a procedure for AuNP synthesis.

3.3 Preparation of filter paper disk

The filter paper sheet was cut into 5-mm diameter circles by using hole puncher prior to use.
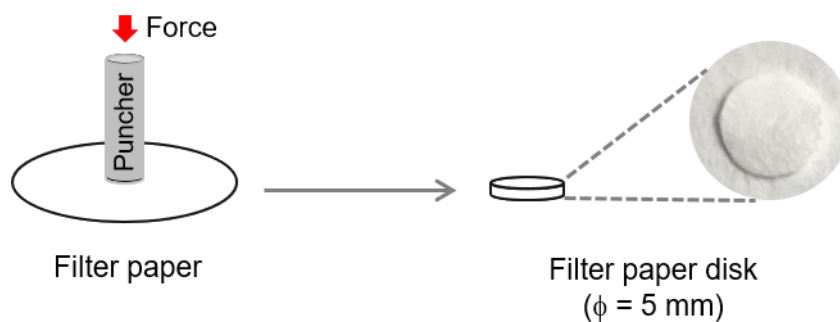
Figure 3.2   A schematic illustrates filter paper disk preparation.

3.4 Fabrication of AuQNP/filter-paper SERS substrate

The fabrication of AuQNP/filter paper is depicted in Figure 3.3. The synthesis of AuQNP on filter paper was produced by our developed method with some modifications [25, 38]. A mixture of tetrachloroauric acid, hydrogen peroxide and silver nitrate was used as a growth solution to prepare AuQNP at room temperature. For direct growth AuQNP/filter paper, the filter paper was immersed in colloidal AuNPs (0.5 M, 2 mL). The AuNP-modified filter paper (AuNP/filter paper) was washed with milli-Q water. $HAuCl_4$ solution (8.3 mM) was dropped on AuNP/filter paper. Then, 6 µL of $AgNO_3$ (66.7 µM) in H_2O_2 (1 M) was dropped on the surface of AuNP/filter paper. The reaction was left for 5 minutes at room temperature, and the color changed from red to purple. Then the substrate was washed with milli-Q water. Finally, the modified-filter paper (AuQNP/filter paper) were washed with NH_4OH and thoroughly rinsed with milli-Q water before further characterization.
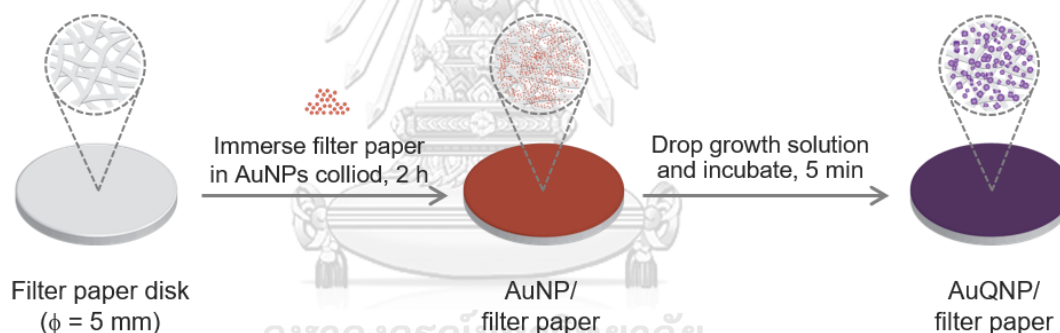
Figure 3.3 A schematic illustrates the fabrication of AuQNP/filter-paper SERS substrates.

3.5 Preparation of BCNC and BCNC-coated filter paper

BCNC was prepared by HCl acid hydrolysis[45], as shown in Figure 3.4. Small cubes of bacterial cellulose pellicles were ground into cellulose paste using a kitchen blender. The cellulose paste was alkaline treated and bleached by NaOH and H_2O_2, respectively. The bleached cellulose was rinsed with water until pH becomes 7 (neutral) before hydrolyzing with HCl (1 M) under stirring and heating for 2 h. The BCNC products were washed repeatedly and dispersed in milli-Q water to give BCNC colloid at pH 7 (neutral). BCNC colloid (0 - 0.8% w/v, 15 µL) was dropped

on the 5-mm diameter filter paper and dried under ambient condition, as shown in Figure 3.5.
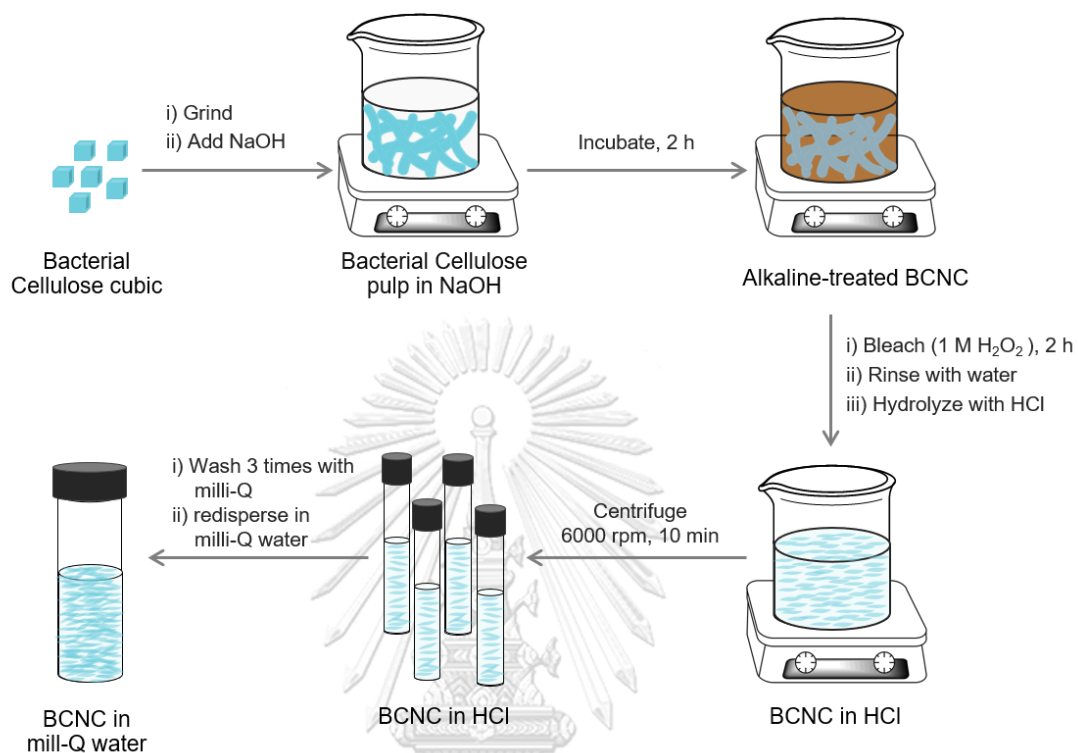
Figure 3.4   A schematic shows a procedure for BCNC colloid preparation.
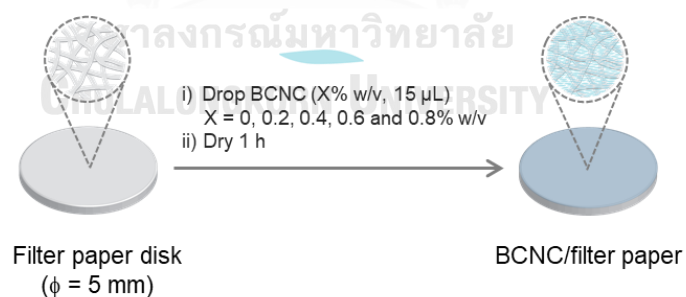
Figure 3.5   A schematic shows a procedure for BCNC/filter paper preparation.

3.6 Fabrication of AuQNP/BCNC/filter-paper SERS substrate

BCNC/filter paper was immersed in colloidal AuNPs (0.5 M, 2 mL). AuNP/BCNC/filter paper was washed with milli-Q water. $HAuCl_4$ solution (8.3 mM) was dropped on AuNP/BCNC/filter paper and followed by 6 µL of $AgNO_3$ (66.7 µM) in H_2O_2 (1 M) solution. The reaction was left for 5 minutes at room temperature, then the substrate was washed with milli-Q water. Finally, the modified-BCNC/filter paper (AuQNP/BCNC/filter paper) was washed with NH_4OH and thoroughly rinsed with milli-Q water before further characterization. The scheme of AuNP/BCNC/filter paper fabrication is demonstrated in Figure 3.6.

Immerse BCNC/filter paper in AuNPs colliod, 2 h

i) add $HAuCl_4$ (8.3 mM)
ii) add 6 µL of $AgNO_3$ (66.7 µM) in H_2O_2 (1 M)
iii) Incubate, 5 min

BCNC/
filter paper

AuNP/BCNC/
filter paper

AuQNP/BCNC/
filter paper
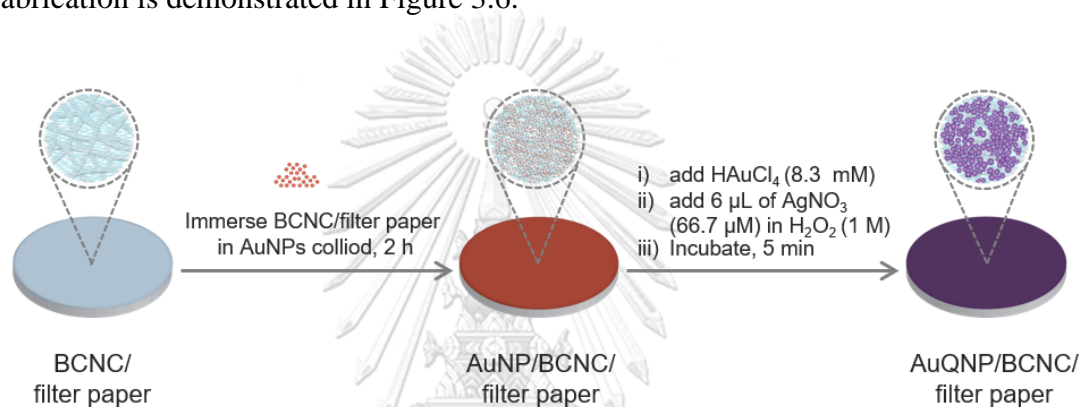
Figure 3.6 A schematic diagram showing the fabrication process of AuQNP/BCNC/filter-paper SERS substrates.

3.7 Characterization techniques

3.7.1 UV-Visible spectroscopy

To measure the plasmon extinction of AuNPs, a plastic cuvette was used as a sample container. Milli-Q water was used as blank. Plasmon extinction spectrum of AuNPs was obtained using GENESYS 10S UV-Vis spectrometer in 400 - 800 nm range.

3.7.2 Infrared spectroscopy

The molecular characteristics of filter paper, bare BCNC and BCNC/filter paper were investigated by infrared (IR) spectroscopy. IR spectra were collected by using ATR FT-IR spectrometer in the range of 500 - 4000 cm^{-1}.

3.7.3 Optical microscopy

To observe the change in the fabrication process of the substrate, the substrate was fixed onto a glass slide and then put on the slot of Ziess optical microscope consisting of 5X, 10X, 20X, 50X and 100X interchangeable of objective lens and a pair of 10X eyes piece.

3.7.4 Field emission scanning electron microscopy

The deposition of AuNPs and AuQNP on substrates was observed by field emission scanning electron microscope (FESEM, JEOL JSM-7610F) operated at 5 kV.

3.7.5 Scanning electron microscopy

The morphology of the AuQNPs and the surface of filter paper, BCNC/filter paper, AuQNP/filter paper and AuQNP/BCNC/filter paper substrate were investigated by scanning electron microscopy (SEM) technique. Samples were fixed on a carbon tape and attached on an aluminium stub. The SEM sample was vacuum dried for 1 h before imaging. SEM micrographs of samples were performed using a scanning electron microscope (SEM, JEOL JSM-6510) operated at 2 - 30 kV under high vacuum mode.

3.7.6 Transmission electron microscopy

The morphology of AuNPs and BCNC was investigated by transmission electron microscopy (TEM, Hitachi Model H-7650). Samples were dropped on a TEM grid and dried in a desiccator for 24 h before measurement.

3.7.7 Raman scattering spectroscopy

To examine the SERS substrate, 4-ATP was utilized as an analyte. The substrate was soaked in 4-ATP solution of known concentration for 24 h. SERS measurements were performed after solvent evaporation. Raman measurements were collected by DXR Raman microscope using 780-nm excitation laser (laser power 7 mW). The acquisition parameters were 10X objective, spot size of 3.1 µm, and 50 µm slit.

CHAPTER 4

RESULTS AND DISCUSSION

4.1 Characterization of gold nanoparticles (AuNPs)

AuNPs were synthesized using tri-sodium citrate dehydrate as a reducing agent [46]. The plasmonic extinction spectrum of the AuNP colloid showed the characteristic peak at ~520 nm as shown in Figure 4.1A. TEM micrograph showed that the particles were close to spherical and uniform size (Figure 4.1B). The size distribution of AuNPs was 15.2 ± 1.3 nm, as determined by TEM (Figure 4.1C). This AuNP size (~15 nm) has a potential to enhance Raman intensity for SERS application [34, 35]. Growing suitable size of particle and packing density with nanoscale gaps will be more effective [36, 37]. Therefore, we attempted to increase the gold nanoparticles size for enhancing Raman intensity by fabricated on paper-based substrate.
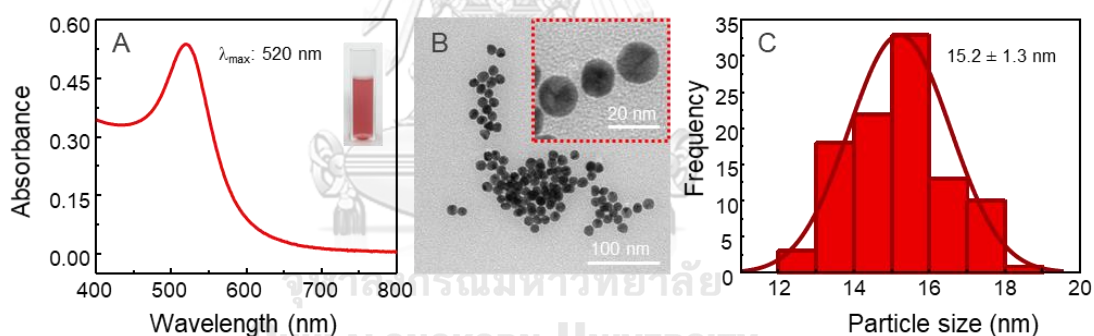
Figure 4.1   (A) The plasmonic extinction spectrum of the synthesized AuNPs colloid (inset: the red wine colloid of AuNPs). (B) TEM micrograph of AuNPs. (C) Particle size of AuNPs.

4.2 Fabrication of AuQNP/filter-paper SERS substrate

4.2.1 Fabrication and SERS testing of AuQNP/filter paper

The AuQNP/filter paper was fabricated by direct growth AuQNP from AuNP (~15 nm) as seeds on filter paper via seed-growth method, as shown in Figure 4.2. The synthesis of AuQNP on filter paper was produced using our developed method with some modifications [25, 38, 47]. AuNPs were used as seeds with filter paper as a substrate-based, hydrogen peroxide as reducing agent and silver ion as catalyst and enhancer of the nucleation process. The filter paper was immersed in AuNPs colloid for 2 h while the concentration of H_2O_2, $HAuCl_4$, and $AgNO_3$ at 1 M, 8.3 mM, and 66.7 µM was used, respectively (more detail was shown in appendix Figure S1 - S4). In the synthesis process, the filter paper (Figure 4.2A) was immersed in a colloidal solution of AuNPs. The color changed from white to red, which indicated the deposition of AuNPs on the surface of the filter paper (Figure 4.2B). The $HAuCl_4$ solution was dropped on the surface, followed by $AgNO_3$ in H_2O_2 solution. In this step, gold ions were reduced to AuNP and grown onto the seed which showed a change from red to dark purple color, as shown in Figure 4.2C. The color changes on the surface were the results of changes on the particle size and density, which also changed the optical property (surface plasmon resonance). This observation corresponded to previous reports where the surface color was changed from red to purple caused by an increase of size and density of particles [21, 48]. It might be indicated that the particle size was increased and gaps between particles were decreased as expected.
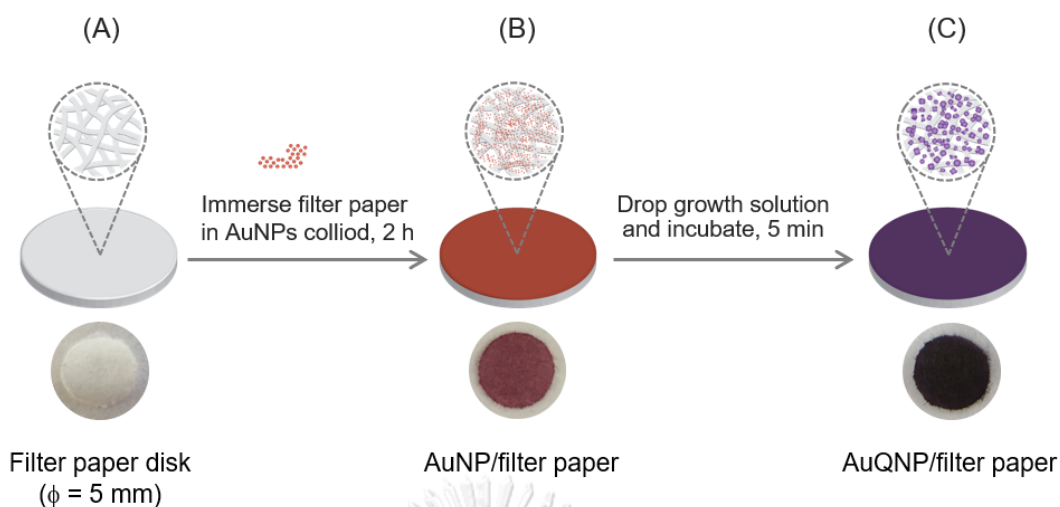
Figure 4.2 Schematic diagram with photograph of substrate illustrates the fabrication of AuQNP/filter-paper SERS substrates; (A) filter paper, (B) AuNP/filter paper and (C) AuQNP/filter paper.

In order to study the SERS activity of the AuQNP/filter paper, the Raman spectra of filter paper, AuNP/filter paper and AuQNP/filter paper without analyte were collected at 780 excitation wavelength, as shown in Figure 4.3A. The Raman spectra of these substrates show a relatively low Raman intensity. From this result, it could be assumed that all of these substrates did not interfere with the analyte signal.

To investigate the influence of metal nanostructure on the Raman signal enhancement of SERS substrate, the filter paper, AuNP/filter paper and AuQNP/filter paper substrate were loaded with 1 µM of 4-ATP as analyte. After 4-ATP molecules were immobilized, the Raman spectra were collected. Figure 4.3B shows the normal Raman of solid 4-ATP and SERS spectra of 4-ATP adsorbed on filter paper, AuNP/filter paper, and AuQNP/filter paper substrate at 780 excitation wavelength. The Raman spectrum of solid 4-ATP exhibited strong bands at 386 cm^{-1} (C-S bending), 471 cm^{-1} (C-S bending) and 1086 cm^{-1} (C-S stretching) and 1593 cm^{-1} (C-C stretching), as shown in Table 4.1 [35, 49]. However, when 4-ATP molecules were adsorbed on the surface of AuQNP/filter paper, the signal of 4-ATP was shifted because of the thiol group (-SH) of 4-ATP, which was chemically bonded to the gold surface. The peak was shifted due to molecular interactions [49]. Considering the peak at 1079 cm^{-1} of 4-ATP, the Raman signal obtained from the filter paper was weak but it was slightly increased

in AuNP/filter paper. Because AuNPs in AuNP/filter paper provided a strong electric field which can enhance the SERS signal compared to filter paper. AuQNP/filter paper generated stronger SERS signals than AuNP/filter paper. The intensity of 4-ATP was increased 8-fold compared to that of the AuNP/filter paper. The observation was consistent with Hong *et al.* reported that too small particle size provided weak SERS enhancement activity due to its low electric field when compared to larger particle size [35]. It was indicated that an increased particle size of AuQNPs growth affected to enhance Raman signal for SERS application.
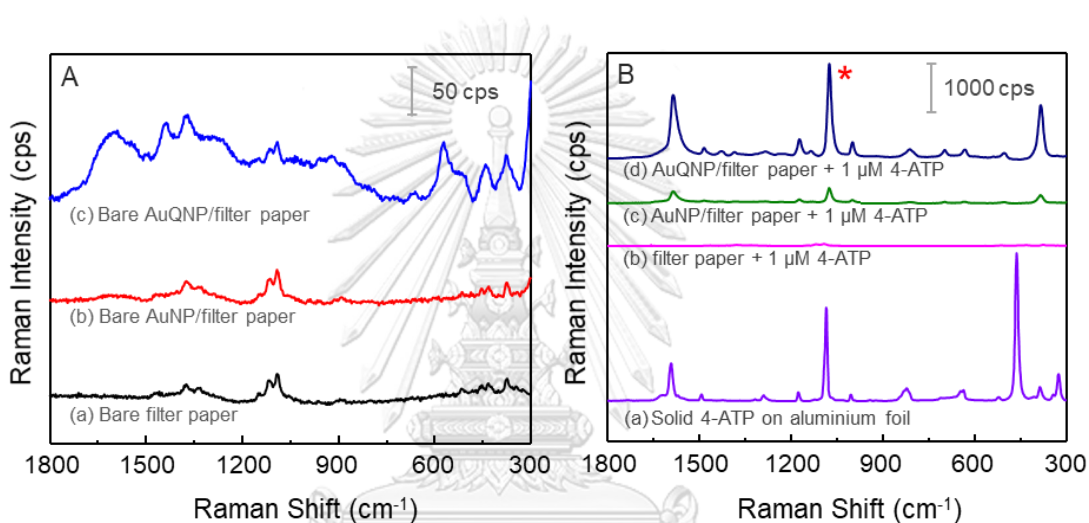
Figure 4.3 Raman spectra of (Aa) bare filter paper, (Ab) bare AuNP/filter paper and (Ac) bare AuQNP/filter paper. (Ba) Raman spectrum of solid 4-ATP on aluminium foil and SERS spectra of μM 4-ATP on (Bb) filter paper, (Bc) AuNP/filter paper, and (Bd) AuQNP/filter paper. Noted: The substrate signal (Figure A) was significantly lower than that of 4-ATP (Figure B).

Table 4.1　Normal Raman of solid 4-ATP position and 4-ATP adsorbed on AuQNP/filter paper substrate position obtained at 780 excitation wavelength.

Peak position of solid 4-ATP (cm^{-1})	Peak position of 1 µM 4-ATP on SERS substrate (cm^{-1})	Band assignment
386	-	C-S bending
471	393	C-S bending
1086	1079	C-S stretching
1593	1582	C-C stretching

4.2.2 An influence of seeds on AuQNP growth for SERS detection

To gain a thorough understanding of the roles of AuNP seeds on the fabrication of AuQNP/filter-paper SERS substrate, we explored the direct growth of AuQNP on the filter paper with seed-growth and without seed-growth modification using similar growth solutions. AuQNP/filter-paper SERS substrates were obtained, as shown in Figure 4.4A - 4.4B. Results showed that the method of seed-growth significantly affected the size and coverage of AuQNP on the substrate. AuQNPs grew and covered the surface of the filter paper causing the gold substrate to appear as shown in Figure 4.4A. Due to the small size of AuQNPs in the substrate with seeds, the morphology and particle size could not be determined under an optical microscope (OM). On the other hand, the particle size of AuQNPs prepared in a condition without seeds were larger and could be observed by naked eyes (Figure 4.4B). Moreover, its low packing density was seen in the changing color of substrate (inset of Figure 4.4A - 4.4B). The case of without seed-growth system exhibited large sizes of AuQNPs on the filter paper due to spontaneous agglomeration between nucleation and growth. The deposited aggregation of AuQNP under without seed-growth system was occurred, making non-uniform deposition of AuQNP on the substrate. This result leaded to gaps between the particles at the micrometer scale, which was not suitable for creating a hot spot for excellent Raman enhancement [9, 37].
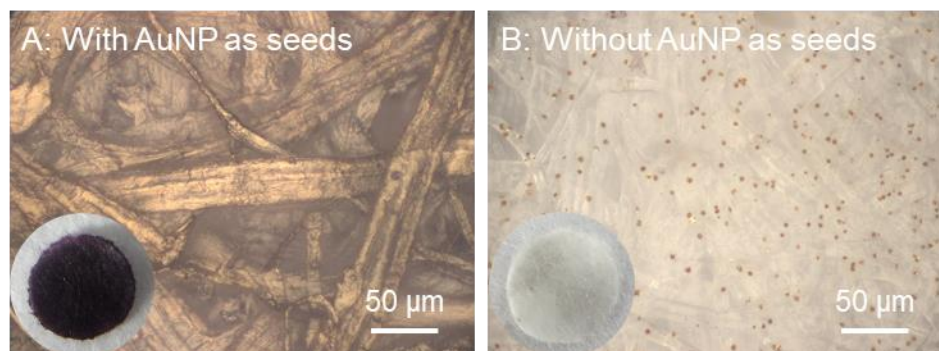
Figure 4.4 Bright-field microscope images (500X magnification) and inset photograph of AuQNP on filter paper synthesized (A) with seed-growth and (B) without seed-growth systems.

SERS activity of AuQNP/filter paper substrates obtained from seed-growth and without seed-growth systems was investigated by using 1 µM of 4-ATP as an analyte, as shown in Figure 4.5A. Both systems acted as potential substrates for SERS enhancement, but AuQNP obtained from seed-growth system provided better results by increasing 7-fold the 4-ATP intensity. Because when the seed-growth system was performed, smaller particle size and narrower inter-particle gaps of AuQNP were obtained compared to the system without seed-growth. This observation was in good agreement with previous reports where the gaps between particles decreased to narrow gaps (nanoscale), enabling even higher Raman signal enhancement [9, 50, 51]. But in case of without seed-growth system, inter-particle gaps of AuQNP is too large (> 5 µm) and non-uniform deposition. So, there was a high variation of hot spots on substrate, resulting in the low enhancement of Raman signal with high fluctuation intensity (Figure 4.5B). Therefore, AuQNP grown with seed-growth system was more effective than that without seed-growth system. As a result, seed-growth was required.
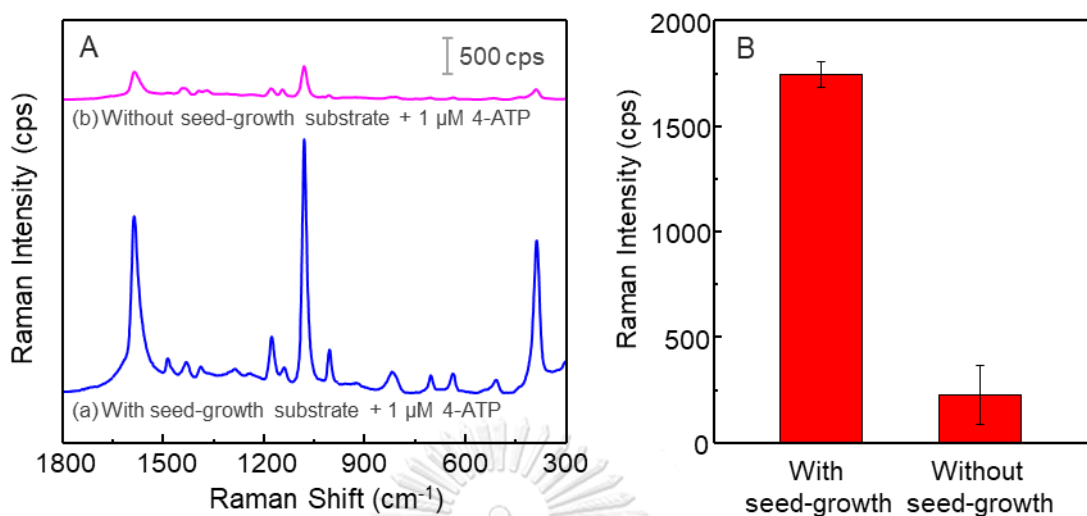
Figure 4.5 SERS spectra of 1 µM 4-ATP on AuQNP/filter paper was synthesized
(Aa) with seed-growth and (Ab) without seed-growth method. (B) SERS
intensity of 4-ATP adsorbed on AuQNP/filter-paper SERS substrate
obtained from seed-growth and without seed-growth systems.

4.2.3 Uniformity SERS signal testing of AuQNP/filter paper

In order to assess the uniform Raman signal enhancement on
AuQNP/filter paper substrate, this substrate was investigated by measuring the SERS
spectra for different 25 spots after applying 1 µM of 4-ATP, as shown in Figure 4.6.
SERS signal with a relative standard deviation (RSD) at 1079 cm^{-1} was obtained at
26.6%, which still showed lower quality than previously reported [52]. Kyudeok *et al.*
reported that SERS substrate with uniform SERS signal could be fabricated with
the RSD lower than 20% [52]. It was indicated that AuQNP/filter paper substrate did
not meet the requirement as uniform SERS signal for practical application. A major
reason of non-uniform SERS signal was due to the variation of the "hot spots", which
was caused by high surface roughness, large pore size and inter-fiber contact of the
filter paper, as shown in Figure 4.7A-B.
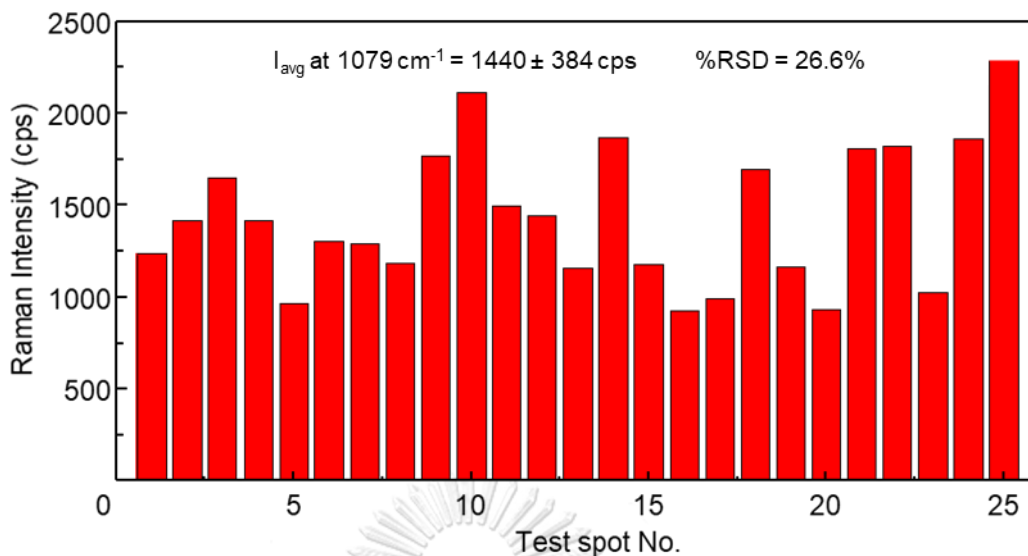
Figure 4.6 SERS signals intensities at 1079 cm^{-1} of 4-ATP (1 µM) on AuQNP/filter paper fabricated by immersing filter paper in AuNP colloid for 2 h. The concentration of H_2O_2, $HAuCl_4$, and $AgNO_3$ at 1 M, 8.3 mM, and 66.7 µM were used, respectively.
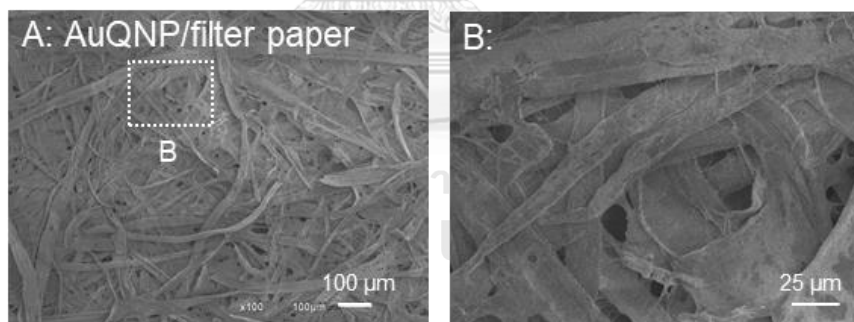
Figure 4.7 SEM images show inter-fiber contact and pores of (A) AuQNP/filter-paper. (B) Higher magnification of (A).

From the above results, high surface roughness of filter paper led to difficulty in creating uniform hot spots and uniform SERS signal. To confirm more clearly, SERS measurement of specific position including fiber and pore area on the AuQNP/filter paper substrate was randomly investigated. Figure 4.8A - 4.8B shows SERS spectra collected from 9 spots on the top layer of fiber and 9 spots of pore,

respectively. The relative standard deviation (RSD) of the SERS signal intensity at 1079 cm^{-1} was calculated to be 18% (Figure 4.8C) and 30% (Figure 4.8D) for the top layer of fiber area and pore area, respectively. From the results, it indicated that, after careful focusing on the fiber and pore area, the smooth fiber surface of the top layer was better uniform SERS signal than a high rough surface of pore area. It can be noticed that the more smoothness surface on fiber, the higher gave a high SERS signal uniformity obtained. Therefore, the filter paper must be modified to produce a smooth surface, which improved the variation of hot spots and non-uniform SERS signals.
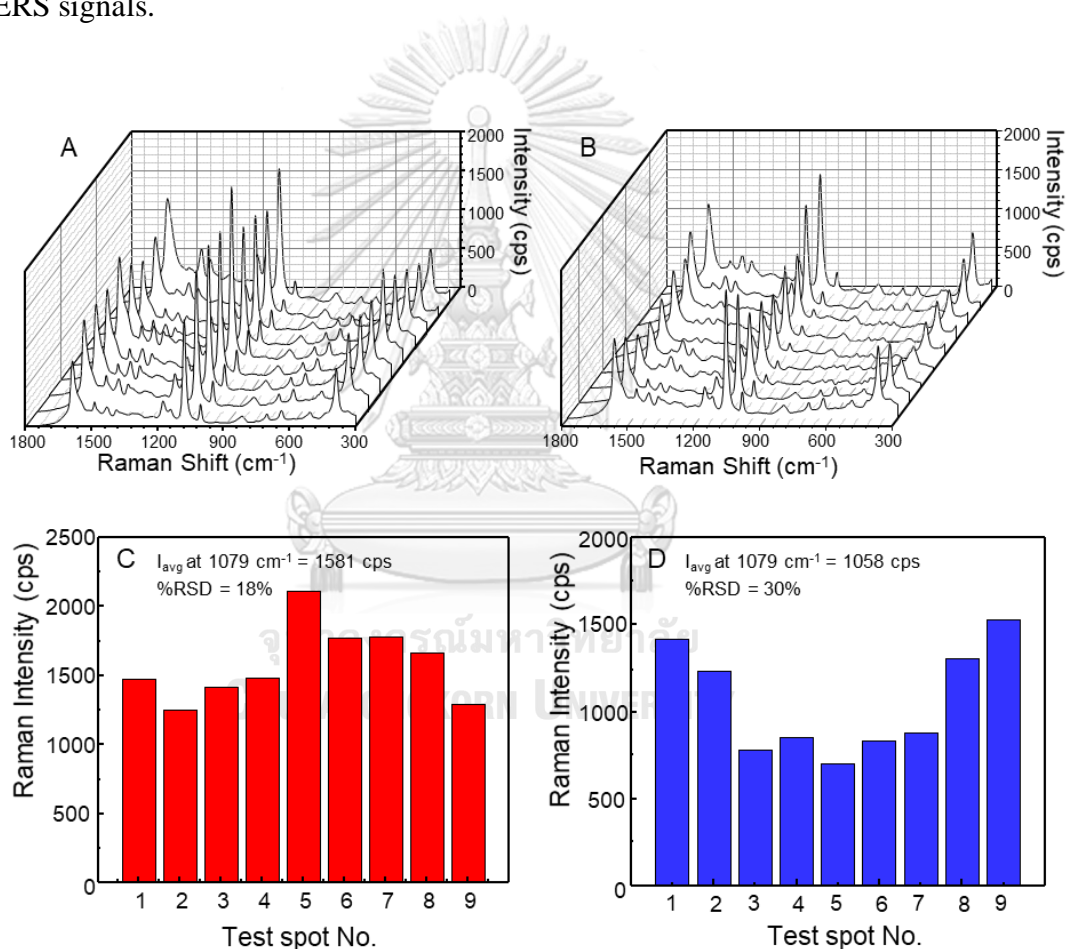
Figure 4.8 SERS spectra of AuQNP/filter paper at random 9 points on (A) fiber and (B) inter-fiber (hole). (C, D) SERS signals intensities of 4-ATP (1 µM) at 1079 cm^{-1} extracted from SERS spectra shown in (A) and (B), respectively.

4.3 Fabrication of AuQNP/BCNC/filter-paper SERS substrate

Recently, nanocellulose has been employed to fill the pore and increase the surface smoothness of the filter paper [43]. Bacterial cellulose nanocrystal (BCNC) is similar to chemical structure of the filter paper [45]. BCNC can be formed as thin, transparent and smooth nanopaper film after drying, as shown in Figure 4.9A. BCNC nanopaper was obtained due to the irreversible collapse of the cellulose nanocrystal network [5, 44]. This represented that BCNC is an interesting material for filter surface modification due to its remarkable chemical and physical properties. So far no one has been currently using BCNC to overcome the smoothness of filter paper roughness. In this work, the BCNC was used to modify the filter paper surface to make it smooth and suitable to grow AuQNPs directly.

Figure 4.9 Photograph of the filter paper and BCNC film placed on a substrate to illustrate the transparency.

4.3.1 Preparation and characterization of BCNC/filter paper

The BCNC colloid solution was homogeneously dispersed and presented a birefringence effect which was a unique property of BCNC (Figure 4.10A). BCNC was HCl-hydrolyzed into short nano-whiskers of 1.93 ± 0.69 µm length (Figure 4.10B - 4.10C). The small size of BCNC colloid was used to smoothen the filter paper surface by filling the pores forming nanopaper thin film on the surface.

SEM was used to characterize the morphology of filter paper and BCNC/filter paper surface. Figure 4.10D shows the surface morphology of filter paper with rough surfaces and large pores. When the filter paper was coated with BCNC,

the surface was smoother and more uniform (Figure 4.10E). The smooth surface would lead to uniform distribution of AuQNPs growth on the BCNC/filter paper substrate.
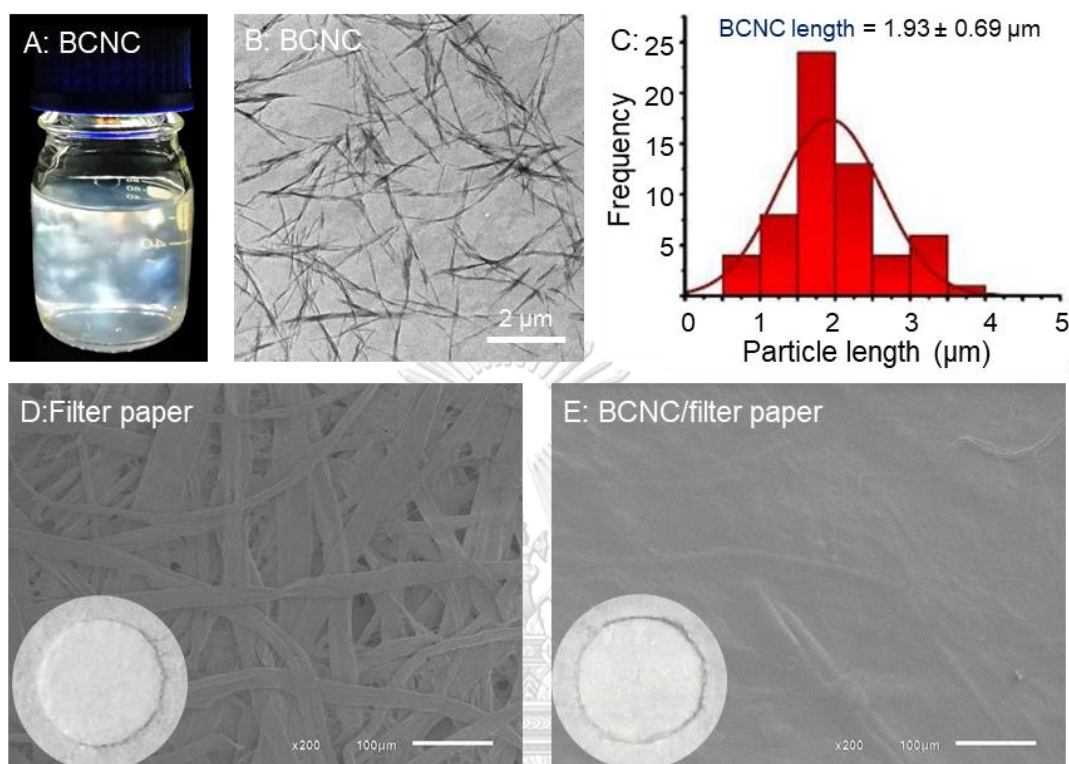
Figure 4.10 (A) BCNC colloid. (B) TEM micrograph of BCNC. (C) particle size of BCNC. SEM micrograph of (D) filter paper (inset: photograph of filter paper) and (E) BCNC/filter paper (inset: photograph of BCNC/filter paper).

To confirm the modification of the surface of the filter paper with BCNC, the molecular characteristics of BCNC on the filter paper were examined by FT-IR spectroscopy. The infrared spectroscopic results of filter paper, BCNC nanopaper and BCNC/filter paper are shown in Table 4.2. The important functional groups are shown in Table 4.2. The vibrational frequencies of the peaks were similar to those previously reported [45, 53]. The vibrational frequencies of the BCNC appeared to be similar to the cellulose of filter paper. However, the significant differences appeared in the crystalline region (3400 - 3200 cm^{-1}) corresponding to OH stretching vibrations. An O-H stretching at 3230 cm^{-1} was observed in only BCNC and was attributed to cellulose I$_\alpha$ which was produced by bacteria [53, 54]. Therefore, this peak could be used to track and indicate that BCNC already covered the filter paper. As can be seen from Figure 4.11, the functional groups presented in the BCNC/filter paper were the same as functional groups in bare BCNC, indicating that BCNC was already covered the filter paper.

Table 4.2 The molecular characteristics of filter paper, bare BCNC and BCNC/filter paper.

Peak position (cm^{-1})			Band assignment
Filter paper	BCNC	BCNC/filter paper	
3331	3341	3341	O-H stretching (intra-chain hydrogen bonding)
3277	3300	3300	O-H stretching vibration of alcohols (intermolecular H-bonds)
-	3230	3230	O-H stretching vibration of alcohols (intermolecular H-bonds)
1427	1427	1427	C-H asymmetric angular deformation of alkane group
1160	1160	1160	C-O-C glycoside bond asymmetric stretching
1106, 1055	1106, 1055	1106, 1055	C-OH stretching in secondary and primary alcohol, respectively
897	897	897	C-H deformation
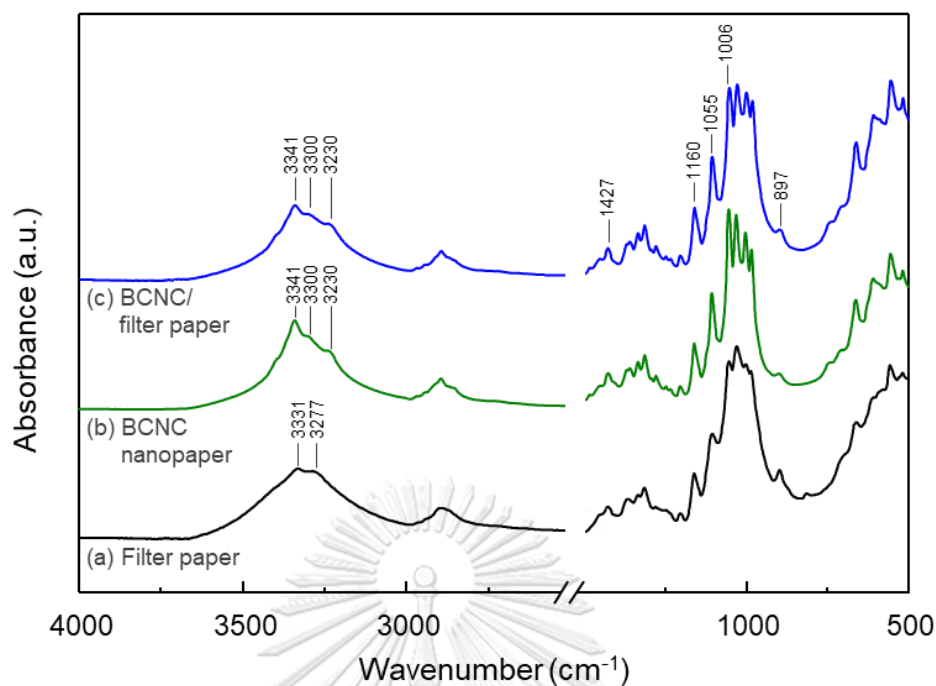
Figure 4.11 IR spectra of bare filter paper, BCNC nanopaper and BCNC/filter paper.

4.3.2 Fabrication and SERS testing of AuQNP/BCNC/filter paper

BCNC colloid was used to smooth the surface by forming into a nanopaper upon drying to fill gaps between fibers. To make sure that the solid content of BCNC in water was sufficient for filling the pore to produce a smooth surface and create uniform hot spots, the optimization of the solid content of BCNC was studied and shown in Figure 4.12.
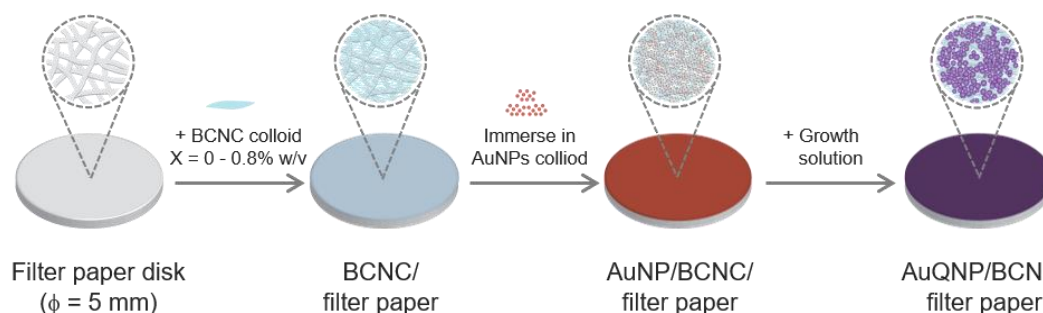
Figure 4.12 Schematic diagram illustrates the fabrication of AuQNP/BCNC/filter-paper SERS substrate. The filter paper was coated with BCNC at 0% w/v, 0.2% w/v, 0.4% w/v, 0.6% w/v and 0.8% w/v solid content of BCNC in water.

BCNC colloid was used to smoothen the filter paper surface by varying the solid content of BCNC in water of 0 - 0.8% w/v. Then, AuQNP was directly grown on BCNC/filter paper via AuNP seeds as previously mentioned in 4.1.1. Briefly, BCNC/filter paper was immersed in AuNP colloid and the color changed from white to red. It is evidence of AuNPs deposited on the BCNC/filter paper surface. The $HAuCl_4$ solution and $AgNO_3$ in H_2O_2 solution were dropped on the surface. The color changed from red to purple, since AuQNP was deposited on BCNC/filter paper. After filter paper was coated with BCNC as thin nanopaper on filter paper, this smooth surface makes AuNPs deposit high efficiently without any lost. The AuQNPs were deposited on the surface and functioned as a creater of hot spots. Based on Figure 4.13A1 - 4.13A3, the smooth surface of BCNC/filter paper shows a uniform AuQNP deposition across the surface. On the other hand, the AuQNP/filter paper revealed non-uniform AuQNPs distribution due to high surface roughness and large pores of filter paper (Figure 4.13B1 - 4.13B3).
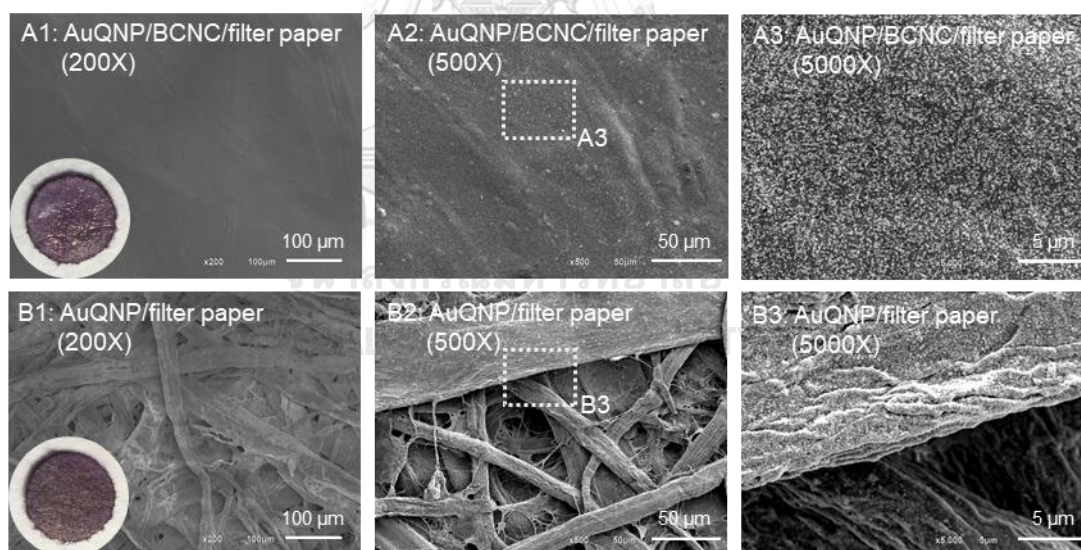
Figure 4.13 SEM image from different magnification of (A1-A3) AuQNP/BCNC/filter paper and (B1 - B3) AuQNP/filter paper.

The uniform SERS signal of AuQNP/BCNC/filter paper was investigated by collecting maps over a 250×250 µm^2 area with 50 µm laser spot intervals after the deposition of 4-ATP (1µM), see appendix Figure S5. The SERS mapping detection of AuQNP/BCNC/filter paper (obtained 0.8% solid content) and AuQNP/filter paper was compared in the same area (Figure 4.14A1 and 4.14B1). The SERS intensity corresponding to 1079 cm^{-1} of 4-ATP was demonstrated in the form of mapping as shown in Figure 4.14A2 and 4.14B2. The different colors from the color chart from green to red were represented the variation of intensity, as shown in Figure 4.14A2 and 4.14B2. The AuQNP/BCNC/filter paper (Figure 4.14A2) gave higher intensity than AuQNP/filter paper (Figure 4.14B2). It might be indicated that smooth surface of AuQNP/BCNC/filter paper helped to create uniform deposition of AuQNP on inter-particle nanogap distance leading to enhance Raman intensity compared to that of filter paper. The representative spectra of three different mapping areas of AuQNP/BCNC/filter paper was similar but the intensity among the spectra was slightly different, as shown in Figure 4.14A3. While three representative spectra from different regions of the AuQNP/filter paper were extremely different intensities (Figure 4.14B3). This confirmed the large variation in the SERS activity over the mapping region. This revealed that the surface treatment of filter paper with BCNC gave much greater SERS intensity and uniformity of SERS signal.
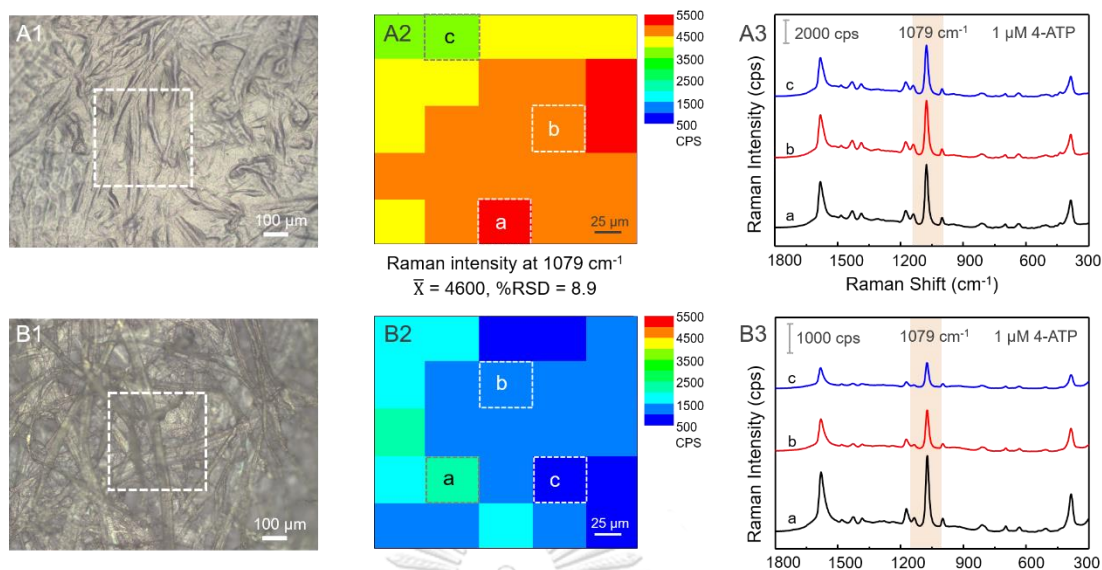
Figure 4.14 Optical images of (A1) AuQNP/BCNC/filter paper and (B1) AuQNP/filter paper. (A2 - B2) The corresponding SERS intensity maps of 4-aminothiophenol (4-ATP) at 1079 cm^{-1} within the selected area. (A3 - B3) Representative SERS spectra of 4-ATP collected from selected position within A2 and B2.

The Raman intensity was calculated for 25 different Raman band of 4-ATP at 1079 cm^{-1} as shown in Figure 4.15A. When the solid content percentages of BCNC in water were increased, the Raman intensity was increased with decreasing of %RSD. After modification of the filter paper above 0.4 % solid content of BCNC in water, the %RSD was below 10% with no significant change (Figure 4.15B). It might be assumed that the pores of substrate which provided high variation of hot spots, were reduced by filling with BCNC. The result led to greater surface smoothness consistent with OM images, as shown in Figure 4.16. Therefore, solid content percentages of BCNC in water of 0.4 - 0.8% w/v were sufficient to make a smooth surface and generate uniform SERS signal. Herein, the AuQNP/BCNC/filter paper that obtained 0.8% solid content of BCNC in water with an acceptable of 8.9% RSD was selected for further study.
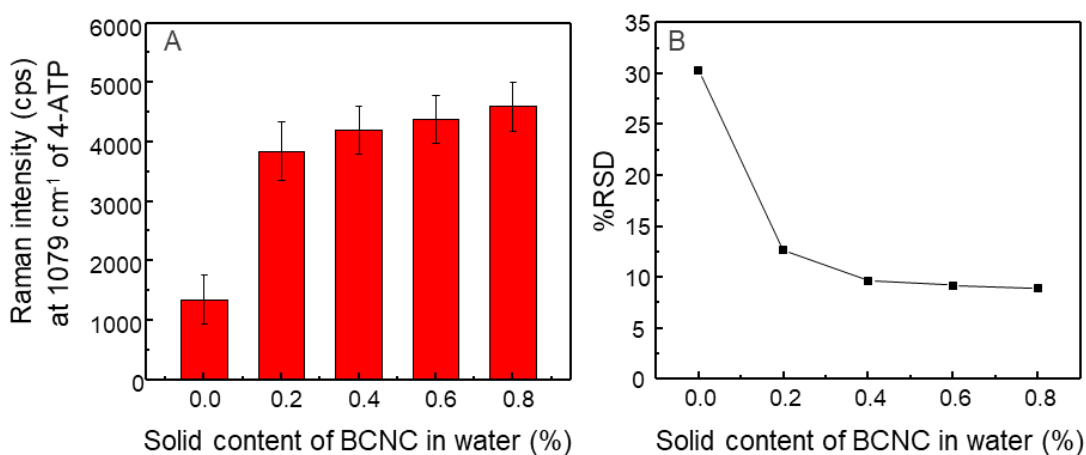
Figure 4.15 The corresponding SERS intensity maps of 4-ATP at 1079 cm^{-1} within the selected area of AuQNP/BCNC/filter paper was fabricated by coating filter paper with different solid content of BCNC in water at 0% w/v, 0.2% w/v, 0.4% w/v, 0.6% w/v and 0.8% w/v: (A) Average SERS intensities and (B) %RSD of SERS substrate at deferent percentage of solid content BCNC in water.
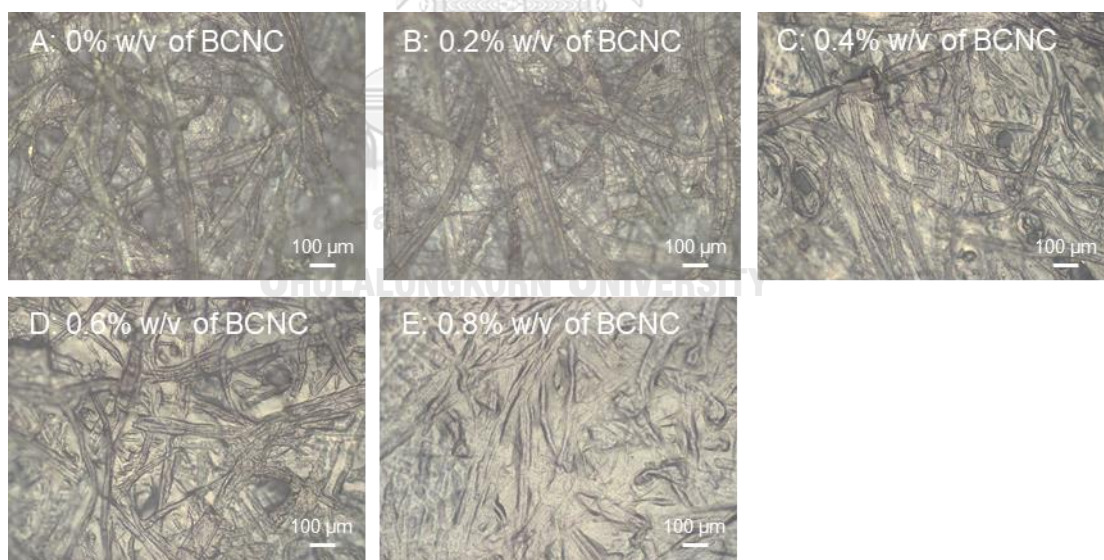
Figure 4.16 Bright-field optical microscope images (200X magnification) of AuQNP fabricated on filter paper substrates that were coated with different solid contents of BCNC in water (A) 0% w/v, (B) 0.2% w/v, (C) 0.4% w/v, (D) 0.6% w/v and (E) 0.8% w/v.

To observe surface morphology of AuQNP/BCNC/filter-paper SERS substrate which was modified by using solid content of BCNC in water at 0.8%, it was investigated by FESEM technique. Figure 4.17A revealed uniform deposition of AuNPs on the BCNC/filter paper without aggregation. AuNPs acted as a seeding for crystal growth. The crystal growth and aggregation led to the formation of AuQNP, as shown in Figure 4.17B. The average size of as-synthesized AuQNP is 65 ± 8 nm. The results show that the surface smoothness substrate helped to improve the uniform decoration of AuNPs (Figure 4.17C) without local aggregation in pores and interfiber contacts. Considering an increase of dense particle packing, the inter-particle distance after seed-growth system was decreased as shown in Figure 4.17D. The uniform growing and packing of AuQNPs were good enough to enhance the Raman scattering intensity.
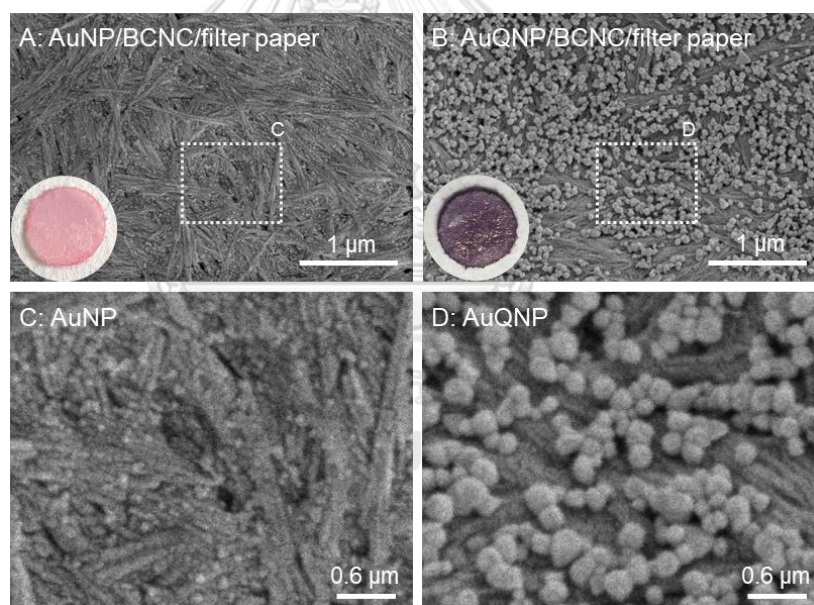
Figure 4.17 FESEM micrographs of (A) AuNP decorated on BCNC/filter paper (inset: photograph of AuNP/BCNC/filter paper) and (B) quasi-spherical gold nanoparticles decorated on BCNC/filter paper (inset: photograph of AuNQP/BCNC/filter paper). (C-D) Higher magnification of (A) and (B), respectively.

SERS activity of AuQNP/BCNC/filter paper was investigated by using 4-ATP as an analyte. The characteristic peaks of BCNC did not interfere with that of the 4-ATP signal. Considering an increase of SERS signals, as shown in Figure 4.18, the observation was in good agreement with previous AuQNP/filter paper reports where a substrate with high electric field has higher SERS signal than a substrate with low electric field. Since BCNC/filter paper did not have an electric field, the Raman signal intensity of bare BCNC/filter paper was weak. While the Raman intensity obtained from AuQNP/BCNC/filter paper was increased about 20-fold compared to that from AuNP/BCNC/filter paper. According to the signal intensity of 4-ATP, AuQNP/BCNC/filter paper produced much stronger electric field than the AuNP/BCNC/filter paper, resulting in enhanced SERS activity as expected. The results were in good agreement with the SEM images. When the particle size was increased, the inter-particle gaps were decreased, resulting in a greater electric field enhancement [32, 55]. This indicated that the particle size and the inter-particle nanogap distance after AuQNP growth played a key role for enhancing Raman scattering intensity.
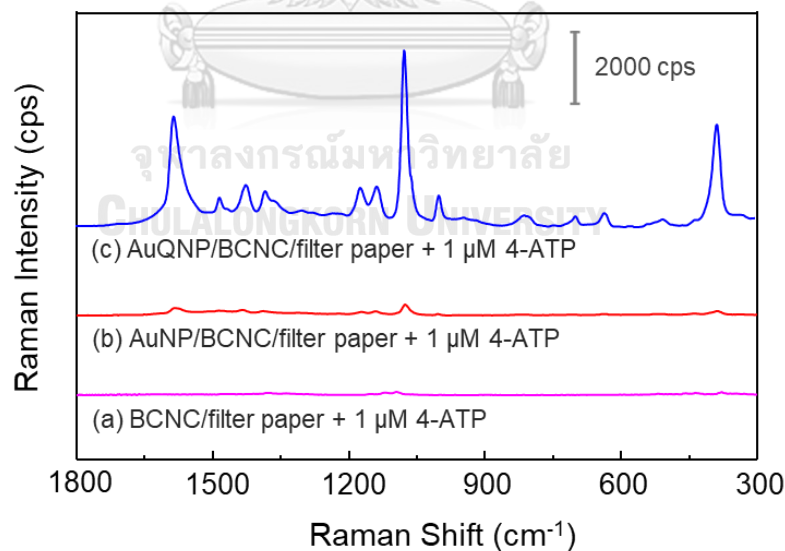
Figure 4.18 SERS spectra of 1 μM 4-ATP on (a) BCNC/filter paper, (b) AuNP/BCNC/filter paper and (c) AuQNP/BCNC/filter paper as SERS substrate.

4.4 SERS performance of the AuQNP/BCNC/filter paper

The developed AuQNP/BCNC/filter-paper SERS substrates were evaluated by measuring the SERS performance with various concentration of 4-ATP. The SERS intensity of the Raman bands of 4-ATP decreased with decreasing 4-ATP concentration. The sensitivity of these SERS substrate was as low as 1 nM (Figure 4.19), revealing excellent sensitivity of the fabricated SERS substrate for trace substance.
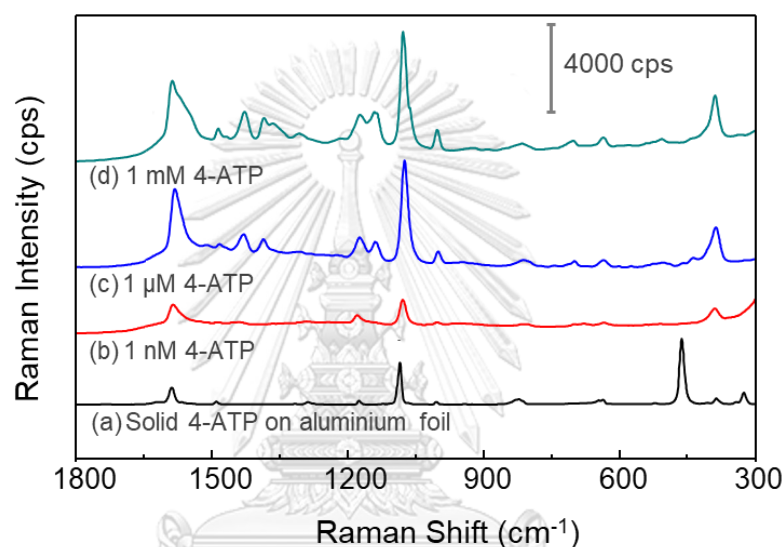
Figure 4.19 (a) Raman spectrum of solid 4-ATP on aluminium foil and SERS spectra of 4-ATP on AuQNP/BCNC/filter paper with concentration of (b) 1 nM, (c) 1 μM, and (d) 1 mM.

4.5 Application for pesticide detection

Thiram is one of the dangerous pesticide residues easily found in fruits and vegetables, therefore, it is necessary to detect this pesticide in the environment. In this study, the obtained AuQNP/BCNC/filter-paper SERS substrates were used to detect different concentrations of thiram in toluene solution from 10 μM to 0.01 pM by using Raman microscopy, as shown in Figure 4.20A-B. The Raman bands of thiram were displayed at 439 cm^{-1} (C=S stretching), 552 cm^{-1} (S-S stretching), 928 cm^{-1} (C=S stretching), 1142 cm^{-1} (C-N stretching), 1378 cm^{-1} (C-N stretching) and 1506 cm^{-1} (C-N stretching) [56, 57]. The most intense Raman peak at 1378 cm^{-1} was

gradually decreased with decreasing thiram concentration. From the higher resolution spectra, the Raman bands corresponding to thiram were clearly distinguishable (signal to noise ratio > 3) down to a concentration of 0.1 pM. As shown in Figure 4.20C, the fitting curve and R^2 value of the SERS intensity of thiram as a function of concentration exhibited a good linear relationship. From the curve and extrapolation calculation suggested that the limit of detection (LOD) equivalent to 0.134 pM, which was more sensitive than previously reported SERS studies [16].
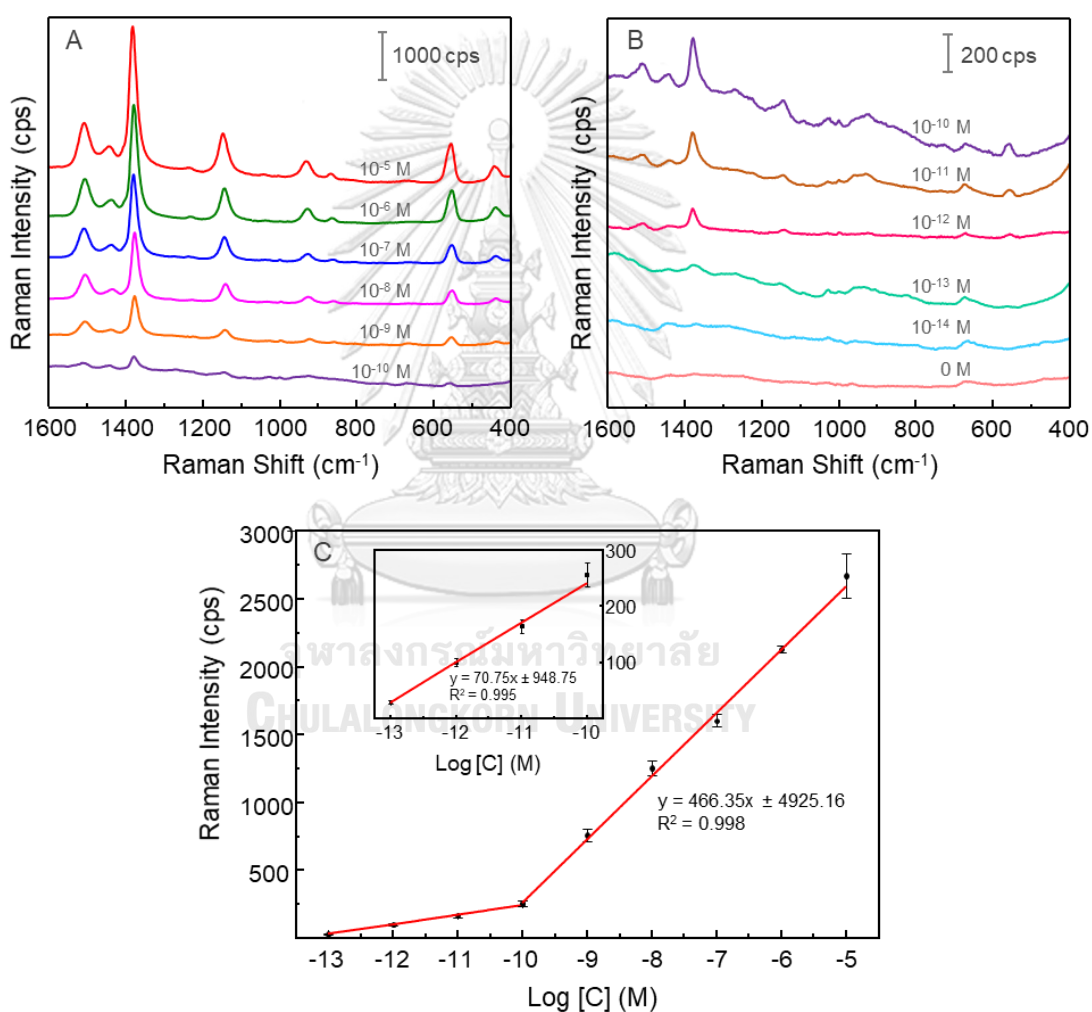
Figure 4.20 SERS detection of thiram pesticide using AuQNP/BCNC/filter paper (A - B) SERS spectra of thiram with different concentration (10 µM to 0.01 pM). (C) Plot of corresponding peak intensities at 1376 cm^{-1} versus the logarithm of thiram concentration.

Figure 4.21 shows the SERS signal intensity mapping of the AuQNP/BCNC/filter paper immersed in 1 nM of thiram. The SERS intensity at 1376 cm^{-1} exhibited uniformity with low RSD of 6.15%. It is important to note that AuQNP/BCNC/filter paper substrate demonstrated a good uniform detection of thiram residues on the substrate. Due to the easy-to-use and high sensitivity, it is therefore concluded that the developed AuQNP/BCNC/filter paper can be used as a SERS sensing platform for practical application.
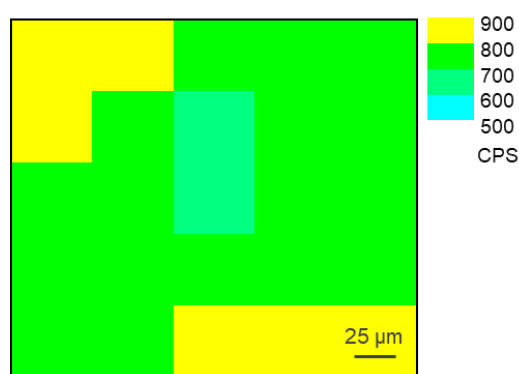
Raman intensity at 1376 cm^{-1}
$\overline{X}$ = 757.74 cps, %RSD = 6.15

Figure 4.21 SERS intensity maps of 1 nM thiram at 1376 cm^{-1} within the selected centre area of AuQNP/BCNC/filter paper.

CHAPTER 5
CONCLUSION

In summary, two filter paper-based SERS substrates were successfully fabricated by direct synthesis of AuQNP on 5-mm diameter of filter paper and BCNC/filter paper. AuQNPs were performed using green chemistry approach by depositing AuNPs on the substrate and directly growing AuQNPs on AuNPs via H_2O_2 reduction of $HAuCl_4$. The AuQNP-decorated filter paper (AuQNP/filter paper) SERS substrate showed good SERS activity. However, AuQNP/filter paper provided fluctuation signal due to irregular hot spots produced by high surface roughness and inter-fiber contact. For this reason, we attempted to improve the surface uniformity of the filter paper by coating the filter paper with bacterial cellulose nanocrystal (BCNC). The BCNC smoothed the surface by forming nanopaper film upon drying while filling the gap between fibers. AuQNPs were synthesized on the surface of BCNC film. The surface smoothness of filter paper resulted in uniform AuQNP distribution. The obtained films of densely packed AuQNP created hot spots which were suitable for sensitive and uniform SERS signals. The AuQNP/BCNC/filter paper was found to be effective and gave uniform SERS signal with acceptable low %RSD (8.9%) compared to AuQNP/filter-paper (RSD = 30.3%). AuQNP/BCNC/filter paper was able to detect a trace amount of 4-ATP as low as 1 nM. Furthermore, this substrate demonstrated the potential to detect trace thiram pesticide with detection limit of 0.134 pM. AQNP/BCNC/filter-paper SERS substrate was a great alternative for SERS sensing in practical application.

REFERENCES

1. Luo, W.; Chen, M.; Hao, N.; Huang, X.; Zhao, X.; Zhu, Y.; Yang, H.; Chen, X., In-situ Synthesis of Gold Nanoparticles on Pseudo-Paper Films as Flexible SERS Substrate for Sensitive Detection of Surface Organic Residues. *Talanta* **2019**, *197*, 225-233.

2. Chen, J.; Huang, M.; Kong, L.; Lin, M., Jellylike Flexible Nanocellulose SERS Substrate for Rapid In-situ Non-Invasive Pesticide Detection in Fruits/Vegetables. *Carbohydrate Polymers* **2019**, *205*, 596-600.

3. Wang, K.; Huang, M.; Chen, J.; Lin, L.; Kong, L.; Liu, X.; Wang, H.; Lin, M., A "Drop-Wipe-Test" SERS Method for Rapid Detection of Pesticide Residues in Fruits. *Journal of Raman Spectroscopy* **2018**, *49* (3), 493-498.

4. Wang, H.; Yao, L.; Mao, X.; Wang, K.; Zhu, L.; Zhu, J., Gold Nanoparticle Superlattice Monolayer with Tunable Interparticle Gap for Surface-Enhanced Raman Spectroscopy. *Nanoscale* **2019**, *11* (29), 13917-13923.

5. Parnsubsakul, A.; Ekgasit, S., Silver Nanoparticle/Bacterial Nanocellulose Paper Composites for Paste-and-Read SERS Detection of Pesticides on Fruit Surfaces. *Carbohydrate Polymers* **2020**, *235*, 115956.

6. Ogundare, S.; Van Zyl, W., A Review of cellulose-based substrates for SERS: fundamentals, design principles, applications. *Cellulose* **2019**, *26*, 6489-6528.

7. Talley, C. E.; Jackson, J. B.; Oubre, C.; Grady, N. K.; Hollars, C. W.; Lane, S. M.; Huser, T. R.; Nordlander, P.; Halas, N. J., Surface-Enhanced Raman Scattering from Individual Au Nanoparticles and Nanoparticle Dimer Substrates. *Nano Letters* **2005**, *5* (8), 1569-1574.

8. Petryayeva, E.; Krull, U. J., Localized Surface Plasmon Resonance: Nanostructures, Bioassays and Biosensing—A review. *Analytica Chimica Acta* **2011**, *706* (1), 8-24.

9. Solís, D. M.; Taboada, J. M.; Obelleiro, F.; Liz-Marzán, L. M.; García de Abajo, F. J., Optimization of Nanoparticle-Based SERS Substrates through Large-Scale Realistic Simulations. *ACS photonics* **2017**, *4* (2), 329-337.

10. Ding, S.-Y.; You, E.-M.; Tian, Z.-Q.; Moskovits, M., Electromagnetic Theories of Surface-Enhanced Raman Spectroscopy. *Chemical Society Reviews* **2017**, *46* (13), 4042-4076.

11. Ye, W.; Wang, D.; Zhang, H.; Zhou, F.; Liu, W., Electrochemical Growth of Flowerlike Gold Nanoparticles on Polydopamine Modified ITO Glass for SERS Application. *Electrochimica Acta* **2010**, *55* (6), 2004-2009.

12. Ko, E.; Hwang, J.; Kim, J. H.; Lee, J. H.; Lee, S. H.; Tran, V.-K.; Chung, W. S.; Park, C. H.; Choo, J.; Seong, G. H., Electrochemical Fabrication of Nanostructures on Porous Silicon for Biochemical Sensing Platforms. *Analytical Sciences* **2016**, *32* (6), 681-686.

13. Su, Q.; Ma, X.; Dong, J.; Jiang, C.; Qian, W., A Reproducible SERS Substrate Based on Electrostatically Assisted APTES-Functionalized Surface-Assembly of Gold Nanostars. *ACS Applied Materials & Interfaces* **2011**, *3* (6), 1873-1879.

14. Fortuni, B.; Fujita, Y.; Ricci, M.; Inose, T.; Aubert, R.; Lu, G.; Hutchison, J. A.; Hofkens, J.; Latterini, L.; Uji-i, H., A Novel Method for In-situ Synthesis of SERS-Active Gold Nanostars on Polydimethylsiloxane Film. *Chemical Communications* **2017**, *53* (37), 5121-5124.

15. He, S.; Chua, J.; Tan, E. K. M.; Kah, J. C. Y., Optimizing the SERS Enhancement of a Facile Gold Nanostar Immobilized Paper-Based SERS Substrate. *RSC Advances* **2017**, *7* (27), 16264-16272.

16. Kim, D.; Ko, Y.; Kwon, G.; Choo, Y.-M.; You, J., Low-Cost, High-Performance Plasmonic Nanocomposites for Hazardous Chemical Detection Using Surface-Enhanced Raman Scattering. *Sensors and Actuators B: Chemical* **2018**, *274*, 30-36.

17. Fierro-Mercado, P. M. H.-R., S. P. , Highly Sensitive Filter Paper Substrate for SERS Trace Explosives Detection. *International Journal of Spectroscopy* **2012**, *2012*, 1-7.

18. Yu, C.-C.; Chou, S.-Y.; Tseng, Y.-C.; Tseng, S.-C.; Yen, Y.-T.; Chen, H.-L., Single-Shot Laser Treatment Provides Quasi-Three-Dimensional Paper-Based Substrates for SERS with Attomolar Sensitivity. *Nanoscale* **2015**, *7* (5), 1667-1677.

19. Zhang, R.; Xu, B.-B.; Liu, X.-Q.; Zhang, Y.-L.; Xu, Y.; Chen, Q.-D.; Sun, H.-B., Highly Efficient SERS Test Strips. *Chemical Communications* **2012**, *48* (47), 5913-5915.

20. Mehn, D.; Morasso, C.; Vanna, R.; Bedoni, M.; Prosperi, D.; Gramatica, F., Immobilised Gold Nanostars in a Paper-Based Test System or Surface-Enhanced Raman Spectroscopy. *Vibrational Spectroscopy* **2013**, *68*, 45-50.

21. Ngo, Y. H.; Li, D.; Simon, G. P.; Garnier, G., Gold Nanoparticle-Paper as a Three-Dimensional Surface-Enhanced Raman Scattering Substrate. *Langmuir* **2012**, *28* (23), 8782-8790.

22. Xiong, Z.; Chen, X.; Liou, P.; Lin, M., Development of Nanofibrillated Cellulose Coated with Gold Nanoparticles for Measurement of Melamine by SERS. *Cellulose* **2017**, *24* (7), 2801-2811.

23. Liou, P.; Nayigiziki, F. X.; Kong, F.; Mustapha, A.; Lin, M., Cellulose Nanofibers Coated with Silver Nanoparticles as a SERS Platform for Detection of Pesticides in Apples. *Carbohydrate Polymers* **2017**, *157*, 643-650.

24. Linh, V. T. N.; Moon, J.; Mun, C.; Devaraj, V.; Oh, J.-W.; Park, S.-G.; Kim, D.-H.; Choo, J.; Lee, Y.-I.; Jung, H. S., A Facile Low-Cost Paper-Based SERS Substrate for Label-Free Molecular Detection. *Sensors and Actuators B: Chemical* **2019**, *291*, 369-377.

25. Pangdam, A.; Wongravee, K.; Nootchanat, S.; Ekgasit, S., Urchin-Like Gold Microstructures with Tunable Length of Nanothorns. *Materials & Design* **2017**, *130*, 140-148.

26. Jang, W.; Byun, H.; Kim, J.-H., Rapid Preparation of Paper-Based Plasmonic Platforms for SERS Applications. *Materials Chemistry and Physics* **2020**, *240*, 122-124.

27. Ding, S.-Y.; Yi, J.; Li, J.-F.; Ren, B.; Wu, D.-Y.; Panneerselvam, R.; Tian, Z.-Q., Nanostructure-Based Plasmon-Enhanced Raman Spectroscopy for Surface Analysis of Materials. *Nature Reviews Materials* **2016**, *1* (6), 16021.

28. Pilot, R.; Signorini, R.; Durante, C.; Orian, L.; Bhamidipati, M.; Fabris, L., A Review on Surface-Enhanced Raman Scattering. *Biosensors (Basel)* **2019**, *9* (2), 57.

29. Guillot, N.; de la Chapelle, M. L., The Electromagnetic Effect in Surface-Enhanced Raman Scattering: Enhancement Optimization Using Precisely Controlled Nanostructures. *Journal of Quantitative Spectroscopy and Radiative Transfer* **2012**, *113* (18), 2321-2333.

30. Wang, K.; Li, S.; Petersen, M.; Wang, S.; Lu, X., Detection and Characterization of Antibiotic-Resistant Bacteria Using Surface-Enhanced Raman Spectroscopy. *Nanomaterials (Basel)* **2018**, *8*.

31. Radziuk, D.; Moehwald, H., Prospects for Plasmonic Hot Spots in Single Molecule SERS Towards the Chemical Imaging of Live Cells. *Physical Chemistry Chemical Physics* **2015**, *17* (33), 21072-21093.

32. Chung, T.; Lee, S.-Y.; Song, E. Y.; Chun, H.; Lee, B., Plasmonic Nanostructures for Nano-Scale Bio-Sensing. *Sensors (Basel)* **2011**, *11* (11), 10907-10929.

33. Kwon, G.; Kim, J.; Kim, D.; Ko, Y.; Yamauchi, Y.; You, J., Nanoporous Cellulose Paper-Based SERS Platform for Multiplex Detection of Hazardous Pesticides. *Cellulose* **2019**, *26* (8), 4935-4944.

34. Hoppmann, E. P.; Yu, W. W.; White, I. M., Highly Sensitive and Flexible Inkjet Printed SERS Sensors on Paper. *Methods* **2013**, *63* (3), 219-224.

35. Hong, S.; Li, X., Optimal Size of Gold Nanoparticles for Surface-Enhanced Raman Spectroscopy under Different Conditions. **2013**, *2013*.

36. Ding, S.-Y.; You, E.-M.; Tian, Z.-Q.; Moskovits, M., Electromagnetic Theories of Surface-Enhanced Raman Spectroscopy. **2017**, *46*.

37. Zhu, W.; Crozier, K. B., Quantum Mechanical Limit to Plasmonic Enhancement as Observed by Surface-Enhanced Raman Scattering. *Nature Communications* **2014**, *5* (1), 5228.

38. Liu, X.; Xu, H.; Xia, H.; Wang, D., Rapid Seeded Growth of Monodisperse, Quasi-Spherical, Citrate-Stabilized Gold Nanoparticles via H_2O_2 Reduction. *Langmuir* **2012**, *28* (38), 13720-13726.

39. Yu, W. W.; White, I. M., Inkjet Printed Surface Enhanced Raman Spectroscopy Array on Cellulose Paper. *Analytical Chemistry* **2010**, *82* (23), 9626-9630.

40. Joshi, P.; Santhanam, V., Paper-Based SERS Active Substrates on Demand. *RSC Advances* **2016**, *6* (72), 68545-68552.

41.   Ngo, Y. H.; Li, D.; Simon, G. P.; Garnier, G., Effect of Cationic Polyacrylamides on the Aggregation and SERS Performance of Gold Nanoparticles-Treated Paper. *Journal of Colloid and Interface Science* **2013**, *392*, 237-246.

42.   Weng, G.; Yang, Y.; Zhao, J.; Zhu, J.; Li, J.; Zhao, J., Preparation and SERS Performance of AuNP/Paper Strips Based on Inkjet Printing and Seed-Mediated Growth: The Effect of Silver Ions. *Solid State Communications* **2018**, *272*, 67-73.

43.   Oh, K.; Lee, M.; Lee, S. G.; Jung, D. H.; Lee, H. L., Cellulose Nanofibrils Coated Paper Substrate to Detect Trace Molecules Using Surface-Enhanced Raman Scattering. *Cellulose* **2018**, *25* (6), 3339-3350.

44.   Tian, L.; Jiang, Q.; Liu, K.-K.; Luan, J.; Naik, R. R.; Singamaneni, S., Bacterial Nanocellulose-Based Flexible Surface-Enhanced Raman Scattering Substrate. *Advanced Materials Interfaces* **2016**, *3* (15), 1600214.

45.   Singhsa, P.; Narain, R.; Manuspiya, H., Bacterial Cellulose Nanocrystals (BCNC) Preparation and Characterization from Three Bacterial Cellulose Sources and Development of Functionalized BCNCs as Nucleic Acid Delivery Systems. *ACS Applied Nano Materials* **2018**, *1* (1), 209-221.

46.   Turkevich, J.; Stevenson, P. C.; Hillier, J., A Study of the Nucleation and Growth Processes in the Synthesis of Colloidal Gold. *Discussions of the Faraday Society* **1951**, *11*, 55-75.

47.   Xia, H.; Bai, S.; Hartmann, J.; Wang, D., Synthesis of Monodisperse Quasi-Spherical Gold Nanoparticles in Water via Silver(I)-Assisted Citrate Reduction. *Langmuir* **2010**, *26* (5), 3585-3589.

48.   Notarianni, M.; Vernon, K.; Chou, A.; Aljada, M.; Liu, J.; Motta, N., Plasmonic Effect of Gold Nanoparticles in Organic Solar Cells. *Solar Energy* **2014**, *106*, 23-37.

49.   Mishra, N.; Liu, M.; Fang, Y.; Kulkarni, S., Study of Adsorption Behavior of Aminothiophenols on Gold Nanorods Using Surface-Enhanced Raman Spectroscopy. **2011**; *5*, 053513.

50.   Compagnini, G.; Galati, C.; Pignataro, S., Distance Dependence of Surface Enhanced Raman Scattering Probed by Alkanethiol Self-Assembled Monolayers.

Physical Chemistry Chemical Physics **1999**, *1* (9), 2351-2353.

51.   Masango, S. S.; Hackler, R. A.; Large, N.; Henry, A.-I.; McAnally, M. O.; Schatz, G. C.; Stair, P. C.; Van Duyne, R. P., High-Resolution Distance Dependence Study of Surface-Enhanced Raman Scattering Enabled by Atomic Layer Deposition. *Nano Letters* **2016**, *16* (7), 4251-4259.

52.   Zhang, P.; Gao, J.; Sun, X., An Ultrasensitive, Uniform and Large-Area Surface-Enhanced Raman Scattering Substrate Based on Ag or Ag/Au Nanoparticles Decorated Si Nanocone Arrays. *Applied Physics Letters* **2015**, *106*, 043103.

53.   Szymańska-Chargot, M.; Cybulska, J.; Zdunek, A., Sensing the Structural Differences in Cellulose from Apple and Bacterial Cell Wall Materials by Raman and FT-IR Spectroscopy. *Sensors* **2011**, *11* (6), 5543-5560.

54.   Yue, Y., A Comparative Study of Cellulose I and II and Fibers and Nanocrystals. **2011**.

55.   Pham, X.-H.; Lee, M.; Shim, S.; Jeong, S.; Kim, H.-M.; Hahm, E.; Lee, S. H.; Lee, Y.-S.; Jeong, D. H.; Jun, B.-H., Highly Sensitive and Reliable SERS Probes Based on Nanogap Control of a Au-Ag Alloy on Silica Nanoparticles. *RSC Advances* **2017**, *7* (12), 7015-7021.

56.   Tang, B.; Zeng, T.; Liu, J.; Zhou, J.; Ye, Y.; Wang, X., Waste Fiber Powder Functionalized with Silver Nanoprism for Enhanced Raman Scattering Analysis. *Nanoscale Research Letters* **2017**, *12*.

57.   Kang, J.-S.; Hwang, S.-Y.; Lee, C.-J.; Lee, M.-S., SERS of Dithiocarbamate Pesticides Adsorbed on Silver Surface; Thiram. *Bulletin of the Korean Chemical Society* **2002**, *23*, 1604-1610.

**APPENDIX**

1. Optimization for AuQNP growth

1.1 The influences of immersion time of filter paper into AuNP seeds

Immersion time of filter paper into AuNPs colliod is one of the parameters affecting the AuQNP growth system thus investigation of seed adsorption behavior is necessary. Time-dependent immersion of filter paper into AuNPs colloid was studied at 1, 2, and 3 h (Figure S1A - C). From OM images, white and red spots are represented as filter paper surfaces and AuNPs, respectively. When the immersion time of filter paper into AuNPs colloid was increased, the surface of the filter paper became darker red, which meant more adsorption of AuNP on the filter paper.
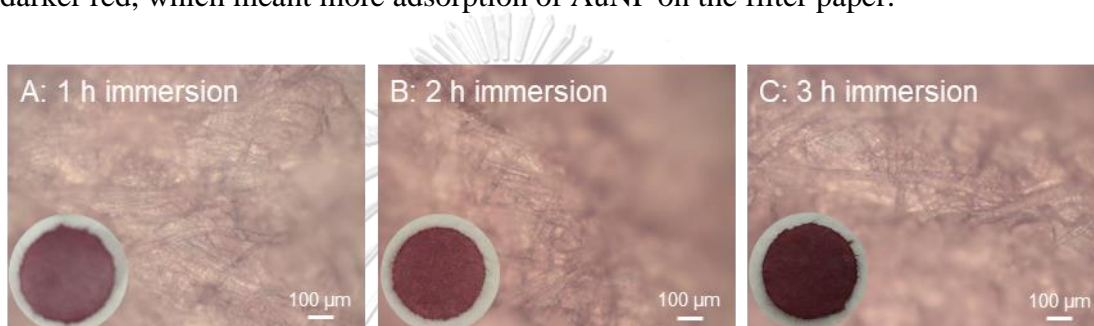
Figure S1 Time-dependent bright-field optical microscope images (200X magnification) of AuNP decoration on filter paper after immersion at (A) 1 h, (B) 2h and (C) 3 h.

In order to examine how long the immersion time of substrates can create the sufficient hot spots to perform the best SERS enhancement, the AuQNP growth from AuNP/filter paper with different time of immersion was investigated as shown in Figure S2A-B. Results showed that the immersion time of AuQNP filter paper substrate from 1 h to 2 h showed an increase of Raman intensity while there was no significant change in 3 h immersion. This might be assumed that 2 h immersion was the suitable particle distribution and inter-particle nanogaps for SERS enhancement. Therefore, AuNPs colloid at 2 h was selected for further study.
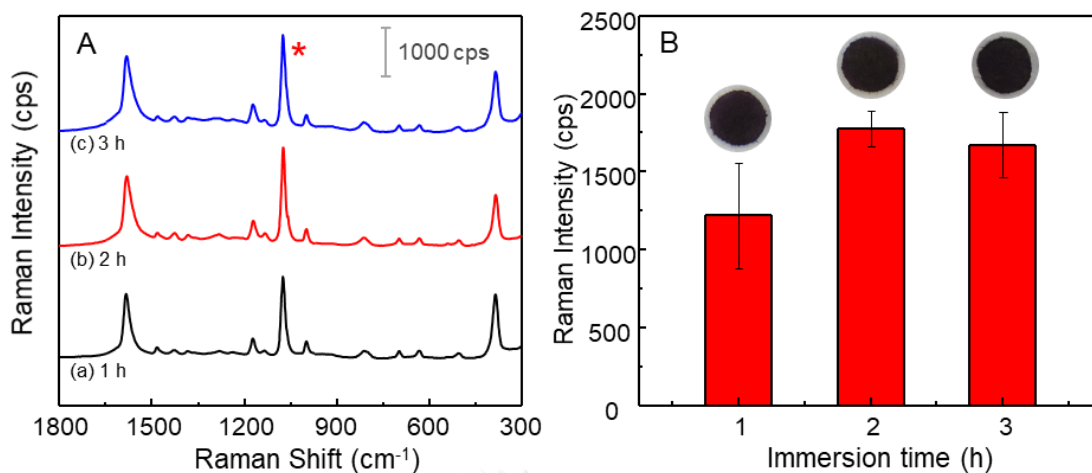
Figure S2 SERS spectra of 1 μM 4-ATP on AuQNP/filter paper was fabricated by immersion time of filter paper in AuNP colloid at (Ab) 1 h, (Ab) 2 h and (Ac) 3 h. (B) SERS intensities of SERS substrate at deferent immersion time in AuNP colloid (inset: photograph of AuQNP/filter paper).

1.2 The influence of silver ion.

To study about the role of Ag^+ in the synthesis system, we explored the optimal concentration of Ag^+ (0 – 133.3 μM) for AuQNP/filter paper fabrication under a fixed concentration of Au^{3+} and H_2O_2 at 8.3 mM and 1 M, respectively. Figure S3 shows the Raman intensity of 4-ATP (1 μM) on AuQNP/filter paper obtained by growth with various concentrations of Ag^+. When the concentration of Ag^+ was increased, the Raman intensity tended to increase. At 66.7 μM Ag^+, the Raman intensity of 4-ATP was increased twice as compared to the substrate without Ag^+. It might be assumed that Ag^+ plays an important role to accelerate the reduction process for AuQNP growth. Finally, 66.7 μM of Ag^+ was selected for further study.
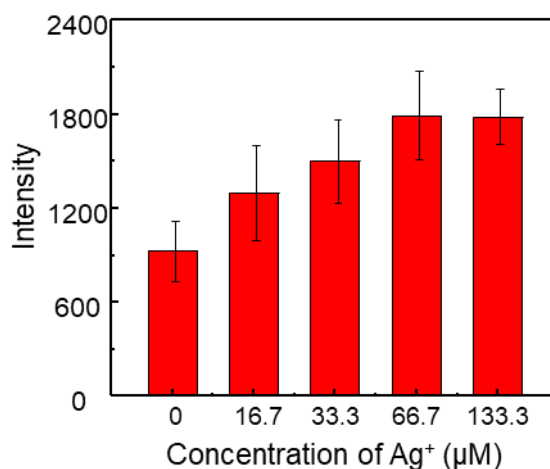
Figure S3   SERS intensities of 1 µM 4-ATP on AuQNP/filter paper fabricated by various concentration of Ag^+ under a fixed concentration of Au^{3+} and H_2O_2 at 8.3 mM and 1 M, respectively.

1.3 The influence of $HAuCl_4$ concentration

For direct growth of AuQNP, the concentration of $HAuCl_4$ were controlled in the range of 4.15, 8.3 and 16.6 mM while the concentration of reducing agent H_2O_2 and Ag^+ were fixed at 1 M and 66.7 µM, respectively. The Raman intensity of 4-ATP was increased when the concentration of Au^{3+} was increased (Figure S4). After AuQNP growth with 8.3 mM Au^{3+}, the Raman intensity of this SERS substrate was insignificantly change. It might be assumed that the obtained substrate at 8.3 mM Au^{3+} provided the sufficient hot spots to fabricate AuQNP/filter-paper SERS substrate. Therefore, the concentration of Au^{3+} at 8.3 µM was used for further study.
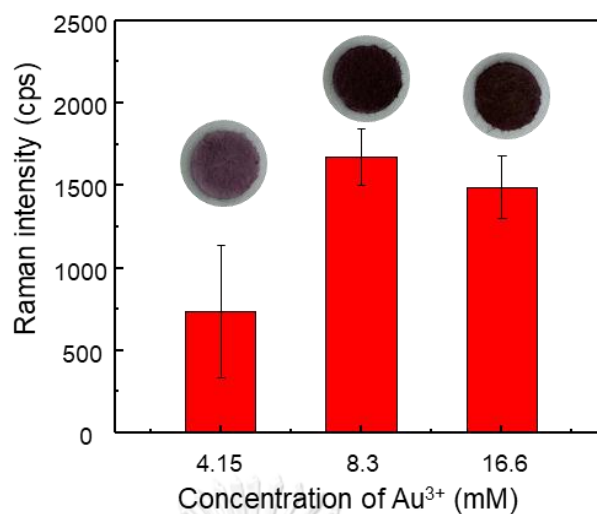
Figure S4 SERS intensities of 1 µM 4-ATP on AuQNP/filter paper fabricated by various concentration of Au^{3+} under a fixed concentration of Ag^+ and H_2O_2 at 66.7 µM and 1 M, respectively.
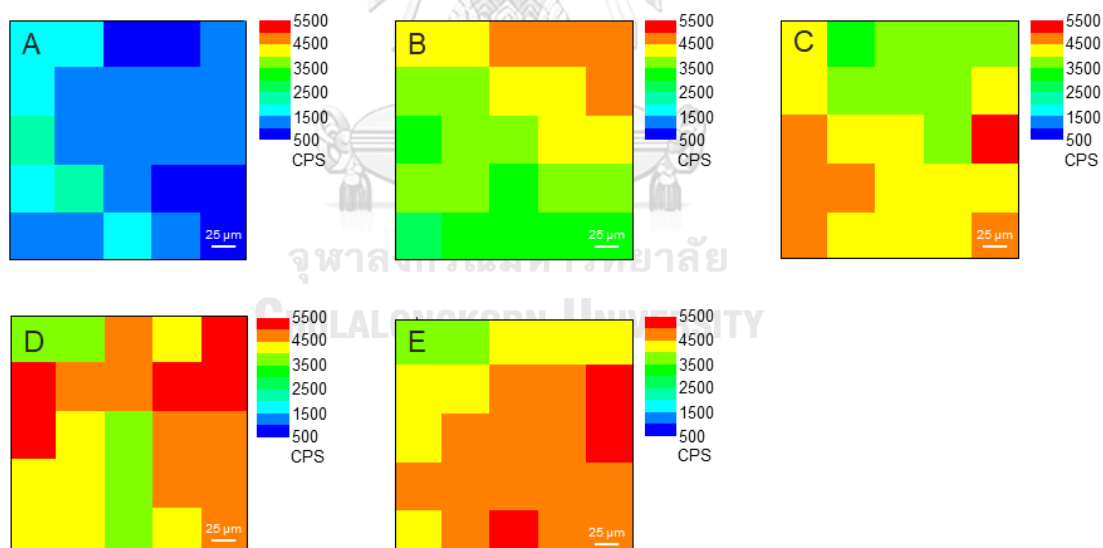
2. SERS testing of AuQNP/filter paper and AuQNP/BCNC/filter paper

Figure S5 SERS intensity maps of 1 nM 4-ATP at 1079 cm^{-1} within the selected area of AuQNP fabricated on filter paper substrate that coating with different solid content of BCNC in water (A) 0% w/v, (B) 0.2% w/v, (C) 0.4% w/v, (D) 0.6% w/v and (E) 0.8% w/v.

VITA

NAME   Piboonwan Insiti

DATE OF BIRTH   08 Sep 1994

PLACE OF BIRTH   Phatthalung

**INSTITUTIONS
ATTENDED**   Chulalongkorn University

HOME ADDRESS   134 Moo. 2 Tanod Duan sub-district, Khua Khanun
                                district, Phatthalung Province 93110

PUBLICATION   Piboonwan Insiti, Attasith Parnsubsakul, Umphan
                                Ngoensawat, Chaweewan Sapcharoenkun, and Sanong
                                Ekgasit,
                                Paper-based SERS Substrate with Improved Signal via
                                Quasi-spherical Gold Nanoparticles Decorated on
                                Bacterial Cellulose Nanocrystal Film, Proceeding of The
                                Pure and Applied Chemistry International Conference
                                2020 (PACCON 2020), Bangkok, Thailand.

AWARD RECEIVED   - Outstanding oral presentation award in The 6th Thailand
                                International Nanotechnology Conference (NanoThailand
                                2018), Entitled "One-step Fabrication of Urchin-like Gold
                                Nanoparticle Film on PDMS Substrates for SERS
                                Applications"
                                - Best poster award (Third Position) in American
                                Association for Advances in Functional Materials
                                (AAAFM)-UCLA International Conference, Entitled
                                "Biocellulose Nanocrystal-Assisted Fabrication of
                                Uniform of Urchin-like Gold Film for Using as SERS
                                Substrate"
                                - Outstanding poster presentation in The Pure and Applied
                                Chemistry International Conference 2020 (PACCON
                                2020), Entitled "Paper-based SERS Substrate with
                                Improved Signal via Quasi-spherical Gold Nanoparticles
                                Decorated on Bacterial Cellulose Nanocrystal Film".